

AVOIDING STABILIZATION TERMS IN VIRTUAL ELEMENTS FOR EIGENVALUE PROBLEMS: THE REDUCED BASIS VIRTUAL ELEMENT METHOD

SILVIA BERTOLUZZA, FABIO CREDALI, AND FRANCESCA GARDINI

ABSTRACT. We present the novel Reduced Basis Virtual Element Method (rbVEM) for solving the Laplace eigenvalue problem. This approach is based on the virtual element method and exploits the reduced basis technique to obtain an explicit representation of the virtual (non-polynomial) contribution to the discrete space. rbVEM yields a fully conforming discretization of the considered problem, so that stabilization terms are avoided. We prove that rbVEM provides the correct spectral approximation with optimal error estimates. Theoretical results are supplemented by an exhaustive numerical investigation.

Keywords: virtual element method, eigenvalue problems, polygonal meshes, error analysis

MSC: 65N15, 65N25, 65N30

INTRODUCTION

Virtual element methods (VEM) are a popular family of numerical schemes originated from mimetic finite difference [7] and allowing for a variational formulation in the spirit of the finite element method, see [8, 3, 6] and references therein. Using VEM, the computational domain can be partitioned by general polytopal meshes, with very minimal shape regularity assumptions. At the element level, the discrete space is defined by considering polynomials up to degree $k \geq 1$ plus additional *virtual* functions, which are not explicitly known since they are solution of a local PDE. Only the polynomial contribution is employed for computing the quantities of interest and ensure the optimal accuracy. On the other hand, the non-polynomial part is only used to enforce the stability of method by introducing a suitable stabilization term [35].

In general, the stabilization term is “artificial” since it does not take into account the physical properties of the problem under consideration. Indeed, it is only required to scale as the virtual (non-polynomial) contribution to the stiffness matrix. It is well-known that the need for the stabilization term may represent a drawback for the method. For instance, defining such term may be non-trivial when dealing with complex nonlinear equations [42], and it may produce inaccurate results when solving anisotropic problems [12].

In order to overcome the difficulties we mentioned above, several recipes have been proposed in literature. The so called *stabilization free* virtual elements [13, 11] enlarge the underlying polynomial space to obtain a discrete formulation which is automatically stable. On the other hand, the *self-stabilized* approach [39, 29, 30] introduces some additional internal degrees of freedom which can be easily condensed. Another option is given by the efficient computation of the virtual functions, which can be pursued by support methods, such as the reduced basis approach [23], neural networks [14], or rational functions [41, 40].

When dealing with eigenvalue problems, the issue of choosing a suitable stabilization term is even more critical since it concerns not only the stiffness matrix, but also the mass term at the right hand side. Indeed, as observed in literature [17, 18], an inappropriate choice of such stabilization terms may introduce additional artificial eigenmodes. In this context, *stabilization free* and *self-stabilized* methods are even more appealing. One option consists in keeping the stabilization term only at the left hand side [2, 19]. Otherwise, fully stabilization-free approaches may be employed in the spirit of [39], as discussed in [36, 33].

In this work, we propose an alternative approach to those mentioned above. We resort to the reduced basis method to efficiently solve the local PDE defining the virtual basis functions as described in [23] for the lowest order VEM. In this way, we obtain an explicit representation of the non-polynomial contribution to the discrete bilinear forms, so that stability is automatically ensured. This new approach results in a fully conforming polygonal method in the spirit of [32], where the VEM machinery is used for dealing with the polynomial part, while the reduced basis method takes care of the non-polynomial contribution. For this reason, we decided to name our approach as *Reduced Basis Virtual Element Method* (rbVEM). We thus derive the variational formulation of the Laplace eigenvalue problem within the rbVEM framework and we carry out the error analysis by proving the correct spectral approximation and optimal convergence estimates. To this aim, a priori error estimates for the source problem are also proved in H^1 - and L^2 -norms. The robustness of our method and its approximation properties are confirmed by a wide range of numerical examples.

The paper is organized as follows. We first recall the continuous formulation of the Laplace eigenproblem in Section 1 and its standard lowest order virtual element discretization in Section 2. Section 3 discusses the construction of the new rbVEM space and introduces the new discrete formulation. The convergence analysis for both the source and the eigenvalue problems is carried out in Sections 4, 5 and 6. Numerical tests confirming our theoretical findings are collected in Section 7. Finally, we draw some conclusions in Section 8.

NOTATION

Throughout the paper we will use standard functional analysis notation. Given an open bounded domain $D \subset \mathbb{R}^2$, we denote by $L^2(D)$ the space of square integrable functions endowed with the scalar product $(\cdot, \cdot)_D$ inducing the norm $\|\cdot\|_{0,D}$. The symbol $H^s(D)$ stands for the family of (Hilbert) Sobolev spaces with differentiability index $s \in \mathbb{R}$, norm $\|\cdot\|_{s,D}$ and semi-norm $|\cdot|_{s,D}$. Moreover $H_0^1(D)$ is the subspace of $H^1(D)$ of functions with zero trace along ∂D . Similarly, $H^s(\partial D)$ denotes the boundary Sobolev space endowed with norm $\|\cdot\|_{s,\partial D}$ and semi-norm $|\cdot|_{s,\partial D}$. The space of continuous functions in D is denoted by $C^0(D)$ with the maximum norm $\|\cdot\|_{\infty,D}$, whereas $\mathbb{P}_k(D)$ stands for the space of polynomials up to degree k in D . Finally, $\mathcal{L}(V, W)$ is the space of linear and continuous operators from V to W , with the simplified notation $\mathcal{L}(V)$ for operators acting from V to itself.

1. PROBLEM SETTING

In this paper, we consider the two-dimensional Laplace eigenvalue problem with homogeneous Dirichlet boundary conditions. Let $\Omega \subset \mathbb{R}^2$ be a polygonal domain, we seek for eigenvalues $\lambda \in \mathbb{R}$ and eigenfunctions $u \neq 0$ satisfying

$$(1) \quad \begin{cases} -\Delta u = \lambda u & \text{in } \Omega, \\ u = 0 & \text{on } \partial\Omega. \end{cases}$$

By testing the equation with $v \in H_0^1(\Omega)$, integration by parts yields the following variational formulation.

Problem 1. *Find $(\lambda, u) \in \mathbb{R} \times H_0^1(\Omega)$, $u \neq 0$, such that*

$$a(u, v) = \lambda b(u, v) \quad \forall v \in H_0^1(\Omega),$$

where

$$a(u, v) = (\nabla u, \nabla v)_\Omega, \quad b(u, v) = (u, v)_\Omega.$$

The bilinear form $a(\cdot, \cdot)$ is continuous and coercive. The above problem admits an infinite sequence of strictly positive eigenvalues

$$0 < \lambda_1 \leq \lambda_2 \leq \dots \leq \lambda_i \leq \dots,$$

which may be repeated accordingly to their multiplicity. It is well-known that such sequence is divergent. Moreover, each λ_i is associated with an eigenfunction u_i satisfying the following properties

$$(2) \quad \begin{aligned} a(u_i, u_j) &= b(u_i, u_j) = 0 & \text{if } i \neq j, \\ b(u_i, u_i) &= 1, \quad a(u_i, u_i) = \lambda_i. \end{aligned}$$

2. THE LOWEST ORDER VIRTUAL ELEMENT METHOD FOR EIGENVALUE PROBLEMS

2.1. The numerical method. We discretize Problem 1 by the lowest order virtual element method. We thus decompose the domain Ω by a mesh \mathcal{T}_h made up of polygons. We denote by $E \in \mathcal{T}_h$ the generic mesh element, having diameter h_E . As usual, the mesh size h corresponds to the maximum of all h_E . Moreover, by abuse of notation, we write $\varepsilon \in \partial E$ meaning that ε is an edge of the element E . We assume standard mesh regularity properties for E (see e.g. [8]), requiring that each E is a star-shaped polygon with respect to a ball of radius $\rho_E \geq Ch_E$ with C being a positive constant. Furthermore, we assume that the edge length is uniformly bounded from below by the diameter, i.e. that there exists a positive constant \tilde{C} , independent of h , such that for all $E \in \mathcal{T}_h$, $|\varepsilon| \geq \tilde{C}h_E$ for all $\varepsilon \in \partial E$.

Before defining the local discrete space, we introduce the elliptic projection $\Pi^\nabla : H^1(E) \rightarrow \mathbb{P}_1(E)$, defined as the unique solution of

$$(3) \quad (\nabla(\Pi^\nabla v - v), \nabla p)_E = 0 \quad \forall p \in \mathbb{P}_1(E), \quad \int_{\partial E} \Pi^\nabla v \, ds = \int_{\partial E} v \, ds.$$

We then consider the *enhanced* virtual element space of order one on E [1], that is

$$(4) \quad V_1(E) = \{v \in H^1(E) : v|_\varepsilon \in \mathbb{P}_1(\varepsilon) \ \forall \varepsilon \in \partial E, \Delta v \in \mathbb{P}_1(E), (\Pi^\nabla v - v, p)_E = 0 \ \forall p \in \mathbb{P}_1(E)\}.$$

The global virtual element space is then easily obtained by glueing together all local spaces by continuity, indeed we have

$$(5) \quad V_h = \{v \in H_0^1(\Omega) : v|_E \in V_1(E) \ \forall E \in \mathcal{T}_h\}.$$

By construction, the inclusion $\mathbb{P}_1(E) \subset V_1(E)$ holds, so that optimal approximation properties are guaranteed. Furthermore, $v \in V_1(E)$ is uniquely determined by its value at the vertices of E , which are a unisolvent set of degrees of freedom. We observe that Π^∇ is well defined on $H^1(E)$ and it is computable through the degrees of freedom when applied to $v \in V_1(E)$. Notice also that the definition of $V_1(E)$ allows also the computation of L^2 -projection $\Pi^0 : V_1(E) \rightarrow \mathbb{P}_1(E)$

$$(6) \quad (\Pi^0 v, p)_E = (v, p)_E \quad \forall p \in \mathbb{P}_1(E).$$

through the degrees of freedom. In particular, the last condition in (4) implies that $\Pi^0 = \Pi^\nabla$. In general, this property is not anymore true if we increase the polynomial degree of the discrete space. In the remainder of the paper, we will keep the two notation distinct.

We now discuss the construction of the discrete problem. We first write the bilinear forms a and b in terms of local contributions, so that

$$(7) \quad \begin{aligned} a(u, v) &= \sum_{E \in \mathcal{T}_h} a^E(u, v), & a^E(u, v) &= (\nabla u, \nabla v)_E, \\ b(u, v) &= \sum_{E \in \mathcal{T}_h} b^E(u, v), & b^E(u, v) &= (u, v)_E. \end{aligned}$$

The projectors Π^∇ provide an orthogonal decomposition of $V_1(E)$ into a polynomial space plus the projection kernel. More precisely, we have

$$(8) \quad V_1(E) = \mathbb{P}_1(E) \oplus V_\perp(E), \quad \text{where } V_\perp(E) = \ker(\Pi^\nabla) \subset V_1(E).$$

Therefore, the splitting of $u_h, v_h \in V_1(E)$ into a polynomial part plus a non-polynomial part gives

$$(9) \quad \begin{aligned} a^E(u_h, v_h) &= a^E(\Pi^\nabla u_h, \Pi^\nabla v_h) + a^E(u_h - \Pi^\nabla u_h, v_h - \Pi^\nabla v_h) \\ b^E(u_h, v_h) &= b^E(\Pi^0 u_h, \Pi^0 v_h) + b^E(u_h - \Pi^0 u_h, v_h - \Pi^0 v_h) \end{aligned}$$

where only the first term at the right hand side of both equations is computable through the degrees of freedom. Such terms ensure the *consistency* of the numerical method. On the other hand, stability is ensured by replacing the non-computable contributions with suitable stabilization terms. Let S_a^E, S_b^E be any two symmetric positive definite bilinear forms scaling as a^E and b^E , respectively

$$(10) \quad \begin{aligned} c_1^* a^E(v_h, v_h) &\leq S_a^E(v_h, v_h) \leq c_1^\sharp a^E(v_h, v_h) \quad \forall v_h \in V_\perp(E), \\ c_2^* b^E(v_h, v_h) &\leq S_b^E(v_h, v_h) \leq c_2^\sharp b^E(v_h, v_h) \quad \forall v_h \in V_\perp(E) \end{aligned}$$

for some positive constants c_i^*, c_i^\sharp for $i = 1, 2$. We then define the local discrete bilinear forms as

$$(11) \quad \begin{aligned} a_h^E(u_h, v_h) &= a^E(\Pi^\nabla u_h, \Pi^\nabla v_h) + S_a^E(u_h - \Pi^\nabla u_h, v_h - \Pi^\nabla v_h), \\ b_h^E(u_h, v_h) &= b^E(\Pi^0 u_h, \Pi^0 v_h) + S_b^E(u_h - \Pi^0 u_h, v_h - \Pi^0 v_h). \end{aligned}$$

The global forms are obtained by summing all local contributions, i.e. $a_h(u, v) = \sum_{E \in \mathcal{T}_h} a_h^E(u, v)$ and $b_h(u, v) = \sum_{E \in \mathcal{T}_h} b_h^E(u, v)$. The discrete problem reads as follows.

Problem 2. *Find $(\lambda_h, u_h) \in \mathbb{R} \times V_h$, $u_h \neq 0$, such that*

$$a_h(u_h, v_h) = \lambda_h b_h(u_h, v_h) \quad \forall v_h \in V_h.$$

Thanks to the stability property, Problem 2 admits $d_h = \dim V_h$ positive eigenvalues

$$0 < \lambda_{1,h} \leq \dots \leq \lambda_{d_h,h}.$$

We denote by $u_{i,h}$ with $i = 1, \dots, d_h$, the corresponding eigenfunctions, satisfying the discrete counterpart of the properties reported in (2). The convergence analysis of the standard virtual element method has been presented in [26].

The stabilization term S_a^E in the definition of the discrete bilinear form a_h is a key ingredient when designing virtual element discretization. Indeed, it guarantees stability and well-posedness of the discrete source problem [8, 1].

When dealing with eigenvalue problems, the mass term $b(\cdot, \cdot)$ appears at the right hand side, posing the issue of its discretization in virtual element framework. A straightforward approach, as discussed above, approximates b by b_h following the same idea as for a_h , namely introducing a second stabilization term S_b^E (see e.g. [37, 10, 38, 26, 25]).

Nevertheless, another approach has been proposed in literature when analyzing the use of virtual elements for the approximation of eigenvalue problems [36, 2, 33, 19]. Such approach consists in dropping the term S_b^E from the definition of the discrete mass term b_h .

In [17], the authors investigated the effect of the stabilization term S_b^E ; in particular, they showed that the choice of the stabilization parameter is critical since it may introduce spurious eigenvalues polluting the discrete spectrum. For the sake of completeness, we briefly recall such results in the next section.

We point out that several options are available for defining the stabilization terms S_a^E and S_b^E , also depending on the problem under consideration, see e.g. [20, 34, 15]. Previous work on the use of virtual elements for eigenvalue approximation follows [17] and make the simplest choice by considering the *dofi-dofi* stabilization: letting $\mathbf{v}_1, \dots, \mathbf{v}_N$ be the vertices of the generic element $E \in \mathcal{T}_h$, this is defined as

$$(12) \quad S_a^E(u_h, v_h) = \sigma_E \sum_{i=1}^N u_h(\mathbf{v}_i) v_h(\mathbf{v}_i), \quad S_b^E(u_h, v_h) = \tau_E h_E^2 \sum_{i=1}^N u_h(\mathbf{v}_i) v_h(\mathbf{v}_i),$$

where σ_E and τ_E are two positive stability parameters, which may depend on E , but not on h . The value of σ_E and τ_E is usually chosen in dependence of the eigenvalues of the local matrices arising from the discretization of $a^E(\Pi^\nabla u_h, \Pi^\nabla v_h)$ and $(1/h_E^2)b^E(\Pi^0 u_h, \Pi^0 v_h)$, respectively.

The aim of the present work is instead to avoid any possible issue regarding the presence of stabilization terms for both discrete bilinear forms. In this direction, we will introduce reduced basis approximation of the nonpolynomial contribution $V_\perp(E)$ to the virtual element space $V_1(E)$, in the spirit of [23], which will allow us to compute the non polynomial component of the splitting (9). This is equivalent to introduce a new discrete space somehow equivalent to the virtual element space (4), which we will leverage for the analysis of the method.

2.2. Parameter-dependent generalized eigenvalue problems in matrix form. In this section we recall the main features of the numerical investigation presented in [17], dealing with the effect of stabilization parameters on the approximation of eigenvalue problems.

To fix ideas, we now assume that $\sigma_E = \alpha$ and $\tau_E = \beta$ in (12) for all polygons $E \in \mathcal{T}_h$. This assumption is reasonable if the parameters σ_E, τ_E vary in a small range.

Due to the presence of the stabilization parameters in (12), and thus in the discrete forms a_h and b_h , it turns out that the algebraic generalized eigenvalue problem

$$(13) \quad \mathbf{K}(\alpha) \mathbf{u} = \lambda \mathbf{M}(\beta) \mathbf{u},$$

arising from Problem 2, is parameter dependent. We point out that $\mathbf{K}(\alpha) = \mathbf{K}_1 + \alpha \mathbf{K}_2 \in \mathbb{R}^{d_h \times d_h}$ represents the stiffness matrix associated with a_h , whereas $\mathbf{M}(\beta) = \mathbf{M}_1 + \beta \mathbf{M}_2 \in \mathbb{R}^{d_h \times d_h}$ is the mass matrix associated with b_h .

Recently, it has been observed that the stabilizing parameters may introduce artificial eigenmodes which pollute the spectrum [17, 18]. In this context, the theoretical results state that, for a given choice of the stabilization parameters, the discrete solution converges to the continuous one with optimal order in h or/and p (see [26, 21]). It is implicitly understood that the convergence depends on the choice of the parameters.

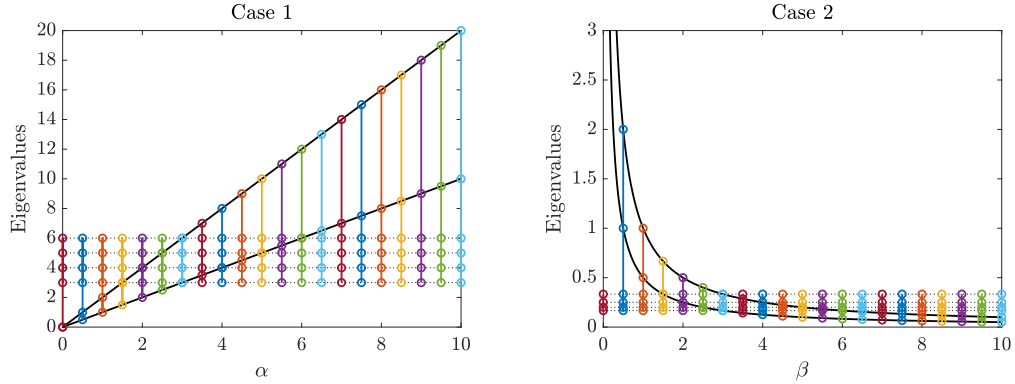


FIGURE 1. Parameters dependence of the eigenvalues.

In [17], under suitable assumptions on K_1, K_2, M_1, M_2 , the authors discuss how the computed spectrum varies in terms of α and β . Moreover, several numerical examples show that the parameters have to be carefully tuned and that wrong choices produce useless results.

More precisely, if only one parameter is varying, the eigenvalues split into two families: a set of eigenvalues depends on such parameter, while all the others are independent. In particular, the dependence on α is linear and thus the corresponding eigenvalues lie on a straight line, while those depending on β lie on hyperbolas. This behavior is depicted in Figure 1, where a simple example is considered. We introduce the matrices $C_1 = \text{diag}([3, 4, 5, 6, 0, 0])$ and $C_2 = \text{diag}([0, 0, 0, 0, 1, 2])$. On the left panel, we set $K(\alpha) = C_1 + \alpha C_2$ and $M = \text{Id}(6)$, so that the eigenvalues are given by $\alpha, 2\alpha, 3, 4, 5, 6$. On the right panel, we set $K = \text{Id}(6)$ and $M(\beta) = C_1 + \beta C_2$, so that the eigenvalues are $1/\beta, 1/(2\beta), 1/3, 1/4, 1/5, 1/6$. It is clear that, in the first case, the eigenvalues depending on α are aligned, whereas in the second case, eigenvalues depending on β lie on hyperbolas.

Even if the matrices arising from the VEM discretization do not completely satisfy the requirements in [17, Assump. 1], numerical tests showed a similar parameters dependence. Choosing a sufficiently large stabilization parameter α and a small (possibly zero) β could be the safest choice. Nevertheless, when $\beta = 0$, the discrete form $b_h(\cdot, \cdot)$ equals the consistency term $b(\Pi^0 \cdot, \Pi^0 \cdot)$, and thus it generally has a nontrivial kernel. In this case, the partially stabilized VEM provides numerical optimal results even if the mass term does not enjoy the stability property. We refer to [19] for the analysis of first and second order VEM approximations of eigenvalue problems when the stabilization parameter β is zero.

Taking into account the above discussion, in order to avoid any dependence of the discrete spectrum on parameters, in this paper we resort to the rbVEM approach introduced in [23] for the source problem.

3. THE RBVEM DISCRETE SPACE

In order to overcome the issues relative to the stabilization forms, we follow the approach introduced in [23], where stability of the discrete source problem is enforced by actually approximating the virtual contribution. We extended such approach to the mass term to deal with eigenvalue problems: this is equivalent to discretize Problem 1 in a different (conforming) space where bilinear forms are fully computable.

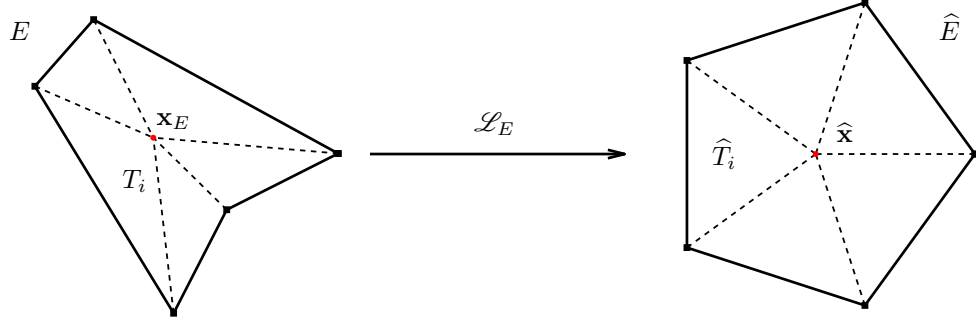


FIGURE 2. An example of affine mapping \mathcal{L}_E between a star shaped pentagon and its reference configuration.

The new discrete space is built upon the virtual element one by means of the Reduced Basis Method, which has been designed for the efficient solution of parametric equations for a large set of parameters. Indeed, we can interpret the family of local problems defining the virtual basis functions on different elements as a geometric parametric problem defined on a reference element.

In this section we introduce the parametric problem and postpone to the Appendix the issue of its efficient solution. We then define the new polygonal discrete space.

Let us consider a generic star-shaped polygon E with N vertices $\mathbf{v}_1, \dots, \mathbf{v}_N$ ordered counter-clockwise. All functions $v \in V_1(E)$ can be written in terms of the nodal basis functions e_1, \dots, e_N , which are solution of the following local PDE.

Problem 3. For $i = 1, \dots, N$, find e_i such that

$$(14) \quad \begin{aligned} -\Delta e_i &= 0 && \text{in } E \\ e_i &= g_i && \text{on } \partial E, \end{aligned}$$

with g_i such that $g_{i|\varepsilon} \in \mathbb{P}_1(\varepsilon)$ for all $\varepsilon \in \partial E$, and $g_i(\mathbf{v}_j) = \delta_{ij}$ for $j = 1, \dots, N$.

Problem 3 can be formulated as a parametric problem on the family of star-shaped polygons with N vertices. To this aim, for fixed N , we rewrite Problem 3 on a reference domain (see, for instance, [28, Chap. 6.2]). Given a polygon E , let $Ker(E)$ denote the set of point for which E is star-shaped and let \mathbf{x}_E and ρ_E being the centroid and the radius of the circumscribed circle, respectively. We then introduce the parameter space

$$(15) \quad \mathcal{P} = \{E : E \text{ polygon with } N \text{ vertices with } Ker(E) \neq \emptyset, \rho_E = 1, \mathbf{x}_E = \hat{\mathbf{x}} = (0, 0)^\top\}.$$

In other words, \mathcal{P} contains all star-shaped polygons with N vertices, centered in the origin, and having circumscribed circle of unit radius.

As reference element, we introduce the regular polygon \hat{E} with vertices $\hat{\mathbf{v}}_1, \dots, \hat{\mathbf{v}}_N$ (ordered counter-clockwise), centered in the origin $\hat{\mathbf{x}} = (0, 0)^\top$. We then construct a piecewise affine map \mathcal{L}_E from the generic E to \hat{E} , as depicted in Figure 2. We decompose both E and \hat{E} into N triangles by connecting their vertices with \mathbf{x}_E and $\hat{\mathbf{x}}$, respectively, i.e.

$$(16) \quad E = \bigcup_{i=1}^N T_i \quad \text{and} \quad \hat{E} = \bigcup_{i=1}^N \hat{T}_i,$$

and we define $\mathcal{L}_E : E \rightarrow \widehat{E}$ as

$$(17) \quad \mathcal{L}_E(\mathbf{x}) = \mathbf{L}_{E,i} \mathbf{x} \quad \text{on } T_i$$

such that

$$(18) \quad \mathcal{L}_E(\mathbf{v}_i) = \widehat{\mathbf{v}}_i, \quad i = 1, \dots, N \quad \text{and} \quad \mathcal{L}_E(\widehat{\mathbf{x}}) = \widehat{\mathbf{x}}.$$

We point out that $\mathbf{L}_{E,i}$ is a 2×2 matrix defined on T_i .

In order to formulate the parametric problem, we first write Problem 3 in variational form and we apply a change of variables, so that we have

$$(19) \quad (\nabla w, \nabla v)_E = \sum_{i=1}^N (\nabla w, \nabla v)_{T_i} = \sum_{i=1}^N \left(|\det(\mathbf{L}_{E,i}^{-1})| \mathbf{L}_{E,i}^\top \mathbf{L}_{E,i} \nabla \widehat{w}, \nabla \widehat{v} \right)_{\widehat{T}_i},$$

where w and v are two generic functions on E . Finally, we introduce the parameter-dependent bilinear form \mathcal{A} defined as

$$(20) \quad \mathcal{A}(\widehat{w}, \widehat{v}; E) = \sum_{i=1}^N \left(|\det(\mathbf{L}_{E,i}^{-1})| \mathbf{L}_{E,i}^\top \mathbf{L}_{E,i} \nabla \widehat{w}, \nabla \widehat{v} \right)_{\widehat{T}_i},$$

hence we obtain the following version of Problem 3, defined on the reference polygon.

Problem 4. *Find $\widehat{e}_i^K \in H^1(\widehat{E})$ such that*

$$\widehat{e}_i^K = \widehat{g}_i \quad \text{on } \partial \widehat{K}, \quad \text{and} \quad \mathcal{A}(\widehat{e}_i^K, \widehat{v}; E) = 0, \quad \text{for all } \widehat{v} \in H_0^1(\widehat{E}),$$

where \widehat{g}_i is the piecewise linear function on $\partial \widehat{E}$ such that $\widehat{g}_i(\widehat{\mathbf{v}}_k) = \delta_{i,k}$ for $i, k = 1, \dots, N$.

In order to solve the parametric Problem 4, we resort to the Reduced Basis Method, see [28] for a survey on its foundations. Such method consists in an offline procedure, where the computational load is concentrated, followed by an efficient online phase, where all computations are carried out on the reference domain making use of pre-computed objects.

We first introduce the piecewise linear finite element space \mathcal{V}_δ defined on a fine (fixed) triangulation \mathcal{T}_δ of \widehat{E} and we reduce Problem 4 to a problem with homogeneous boundary conditions. Thus, we let $\widehat{\Theta}_i \in \mathcal{V}_\delta$ be the discrete harmonic lifting of \widehat{g}_i defined as solution of

$$(21) \quad \left(\nabla \widehat{\Theta}_i, \nabla v_\delta \right)_{\widehat{E}} = 0 \quad \forall v_\delta \in \mathcal{V}_\delta \cap H_0^1(\widehat{E}), \quad \text{with} \quad \widehat{\Theta}_i = \widehat{g}_i \quad \text{on } \partial \widehat{E},$$

so that we can write \widehat{e}_i^K as the sum of two contributions

$$(22) \quad \widehat{e}_i^K = \widehat{\Theta}_i + \widehat{d}_{i,\delta}[E],$$

where $\widehat{d}_{i,\delta}[E]$ is solution of the following parametric problem.

Problem 5. *For $i = 1, \dots, N$, find $\widehat{d}_{i,\delta}[E] \in H_0^1(\widehat{E})$ such that*

$$\mathcal{A}(\widehat{d}_{i,\delta}[E], \widehat{v}; E) = -\mathcal{A}(\widehat{\Theta}_i, \widehat{v}; E) \quad \forall \widehat{v} \in H_0^1(\widehat{E}).$$

The reduced basis approach we designed for efficiently solve Problem 5 has been presented in [23] and it is briefly recalled in the Appendix. In this context, we seek for an approximation $\widehat{d}_{M,i}^{\text{rb}}[E]$ of $\widehat{d}_{i,\delta}[E]$ in a suitable reduced subspace of \mathcal{V}_δ of dimension $M \ll \dim(\mathcal{V}_\delta)$, so that we find

$$(23) \quad \widehat{e}_{M,i}^{\text{rb}}[E] = \widehat{\Theta}_i + \widehat{d}_{i,\delta}^{\text{rb}}[E], \quad i = 1, \dots, N,$$

and, by pull back, we obtain

$$(24) \quad e_{M,i}^{\text{rb}}[E] = \hat{e}_{M,i}^{\text{rb}}[E] \circ \mathcal{L}_E^{-1}, \quad i = 1, \dots, N,$$

which are the reduced basis approximation of the VEM basis functions.

Given $E \in \mathcal{T}_h$, our approach is based on the idea that we can compute exactly the bilinear forms a^E and b^E if we consider the functions $e_{M,i}^{\text{rb}}[E]$ constructed in (24). Then we define a new suitable discrete space V_h^{rb} , where all quantities are computable. We first introduce the boundary space

$$(25) \quad \mathbb{B}^\perp(\partial E) = \left\{ v \in H^{1/2}(\partial E) : \int_{\partial E} v \nabla q \cdot \mathbf{n}^E \, ds = 0 \, \forall q \in \mathbb{P}_1(E), \int_{\partial E} v \, ds = 0 \right\}$$

such that $\Pi^\nabla v = 0$ if and only if $v|_{\partial E} \in \mathbb{B}^\perp(\partial E)$. For fixed M , we then define the RB space

$$(26) \quad W_h^{\text{rb}}(E) = \{v \in \text{span}\{e_{M,1}^{\text{rb}}[E], \dots, e_{M,N}^{\text{rb}}[E]\} : v \in \mathbb{B}^\perp(\partial E)\}$$

and, finally, the new discrete rbVEM space

$$(27) \quad V_h^{\text{rb}}(E) = \mathbb{P}_1(E) \oplus W_h^{\text{rb}}(E).$$

We observe that, by construction, $\mathbb{P}_1(E) \subset V_h^{\text{rb}}(E)$. Moreover, the polynomial contribution to $V_h^{\text{rb}}(E)$ is the result of the action of the operator Π^∇ on the virtual element space $V_1(E)$. In other words, our new space $V_h^{\text{rb}}(E)$ is spanned by the basis functions $\tilde{e}_1^{\text{rb}}, \dots, \tilde{e}_N^{\text{rb}}$ defined as

$$\tilde{e}_i^{\text{rb}} = \Pi^\nabla e_i + \sum_{j=1}^N (e_i(\mathbf{v}_j) - \Pi^\nabla e_i(\mathbf{v}_j)) e_{M,j}^{\text{rb}}[E], \quad i = 1, \dots, N,$$

where e_i are the virtual basis functions of $V_1(E)$.

Let $u_h^{\text{rb}}, v_h^{\text{rb}} \in V_h^{\text{rb}}(E)$, then the following representation holds

$$(28) \quad u_h^{\text{rb}} = u^P + u^W, \quad v_h^{\text{rb}} = v^P + v^W, \quad \text{with } u^P, v^P \in \mathbb{P}_1(E), u^W, v^W \in W_h^{\text{rb}}(E)$$

so that

$$(29) \quad a(u_h^{\text{rb}}, v_h^{\text{rb}}) = a(u^P, v^P) + a(u^W, v^W) + a(u^P, v^W) + a(u^W, v^P)$$

and

$$(30) \quad b(u_h^{\text{rb}}, v_h^{\text{rb}}) = b(u^P, v^P) + b(u^W, v^W) + b(u^P, v^W) + b(u^W, v^P).$$

We observe that due to the orthogonal decomposition of the local rbVEM space $V_h^{\text{rb}}(E)$ with respect to $a(\cdot, \cdot)$, the cross terms $a(u^P, v^W)$ and $a(u^W, v^P)$ vanish. On the other hand, we emphasize that this is not true for $b(u^P, v^W)$ and $b(u^W, v^P)$, which must be considered when assembling the mass matrix. The computability of such terms is not an issue since rbVEM provides all the required information. Algorithm 1 in the Appendix describes how to efficiently construct the matrices arising from Problem 6 by exploiting the properties of VEM and of the Reduced Basis method. We are going to show that the new space $V_h^{\text{rb}}(E)$ satisfies optimal approximation properties and that the solution of Problem 6 is not polluted by spurious eigenvalues.

By glueing all local spaces by continuity, we find the global rbVEM space

$$(31) \quad V_h^{\text{rb}} = \{v \in H_0^1(\Omega) : v|_E \in V_h^{\text{rb}}(E) \text{ for all } E \in \mathcal{T}_h\}.$$

Discretizing Problem 1 in V_h^{rb} by a standard (fully conforming) Galerkin method we obtain the following problem.

Problem 6. Find $(\lambda_h^{\text{rb}}, u_h^{\text{rb}}) \in \mathbb{R} \times V_h^{\text{rb}}$, $u_h^{\text{rb}} \neq 0$, such that

$$a(u_h^{\text{rb}}, v_h^{\text{rb}}) = \lambda_h^{\text{rb}} b(u_h^{\text{rb}}, v_h^{\text{rb}}) \quad \forall v_h^{\text{rb}} \in V_h^{\text{rb}}.$$

Since basis functions are explicitly known, all quantities are computable and stabilization parameters disappear from the discrete problem. We highlight that, by construction, the new discrete space has the same set of degrees of freedom as the original virtual element space. We can then interpret Problem 6 as a different non-conforming formulation of our eigenvalue problem in the virtual element space V_h , of the form

Problem 6(b). Find $(\lambda_h, u_h) \in \mathbb{R} \times V_h$, $u_h \neq 0$, such that

$$a_h(u_h, v_h) = \lambda_h b_h(u_h, v_h) \quad \forall v_h \in V_h,$$

where $a_h : V_h \times V_h \rightarrow \mathbb{R}$ and $b_h : V_h \times V_h \rightarrow \mathbb{R}$ are defined as

$$(32) \quad a_h(u_h, v_h) = \sum_E a_h^E(u_h, v_h), \quad a_h^E(e_i, e_j) = a(\tilde{e}_i^{\text{rb}}, \tilde{e}_j^{\text{rb}}),$$

$$(33) \quad b_h(u_h, v_h) = \sum_E b_h^E(u_h, v_h), \quad b_h^E(e_i, e_j) = b(\tilde{e}_i^{\text{rb}}, \tilde{e}_j^{\text{rb}}).$$

Remark 1. The “virtual element reader” would have probably discretized the eigenvalue problem in a different way by considering the (local) bilinear forms

$$(34) \quad \begin{aligned} a_h^E(u_h, v_h) &= a(\Pi^\nabla u_h, \Pi^\nabla v_h) + S_a^{E,\text{rb}}(u_h^W, v_h^W) & \text{with} & \quad S_a^{E,\text{rb}}(u_h^W, v_h^W) = a^E(u_h^W, v_h^W), \\ b_h^E(u_h, v_h) &= b(\Pi^0 u_h, \Pi^0 v_h) + \chi S_b^{E,\text{rb}}(u_h^W, v_h^W) & \text{with} & \quad S_b^{E,\text{rb}}(u_h^W, v_h^W) = b^E(u_h^W, v_h^W) \end{aligned}$$

with $u_h, v_h \in V_1(E)$, $u_h^W, v_h^W \in W_h^{\text{rb}}(E)$ and $\chi = 0, 1$.

More precisely, $a_h^E(\cdot, \cdot)$ is defined by choosing the RB-stabilization introduced in [23] and the stability parameter is dropped out since we are replacing the non-computable term by its reduced basis approximation. Notice that $a_h^E(\cdot, \cdot)$ is exactly the same bilinear form as in (29), but defined in the original virtual element space $V_1(E)$. The same argument applies to the mass term: indeed, if $\chi = 1$, we stabilize $b_h^E(\cdot, \cdot)$ by a reduced basis approximation of the non-computable part of $V_1(E)$. Unlike the bilinear form in (30), this definition does not contain cross terms. The choice $\chi = 0$ yields to a partially stabilized formulation that is also admissible.

The rb-stab-VEM formulations in (34) fall in the framework of standard VEM, where stabilization terms are only required to scale as the actual non-computable contributions. Optimal convergence properties are thus ensured by the virtual elements theory.

4. SPECTRAL THEORY FOR COMPACT OPERATORS

We first introduce the continuous source problem associated with Problem 1, which reads as follows.

Problem 7. Given $f \in L^2(\Omega)$, find $u \in H_0^1(\Omega)$ such that

$$a(u, v) = (f, v)_\Omega \quad \forall v \in H_0^1(\Omega).$$

It is well-known that the above problem is well-posed and admits a unique solution [31]. Moreover, there exists $1/2 < s \leq 1$ such that $u \in H^{1+s}(\Omega)$ and the following stability estimate holds

$$(35) \quad \|u\|_{1+s, \Omega} \leq C \|f\|_{0, \Omega}.$$

In order to carry out the spectral convergence analysis of our method, we introduce the solution operator $T : H^1(\Omega) \rightarrow H^{1+s}(\Omega) \subset H^1(\Omega)$ defined as $Tf = u$, where u is the unique solution to Problem 7, namely

$$a(Tf, v) = (f, v)_\Omega \quad \forall v \in H_0^1(\Omega).$$

It turns out that such operator is linear, continuous, and self-adjoint. We point out that T is also compact, thanks to the compact embedding of $H^{1+s}(\Omega)$ in $H^1(\Omega)$. Moreover, there is a one-to-one correspondence between eigenpairs of Problem 1 and those of T . Indeed, if (λ, u) is an eigenpair for the continuous Problem 1, then $(1/\lambda, u)$ is an eigenpair for T , and viceversa.

Similarly, we now introduce the discrete source problem associated with Problem 6, with both bilinear form a and right hand side discretized by the rbVEM approach.

Problem 8. Given $f \in L^2(\Omega)$, find $u_h^{\text{rb}} \in V_h^{\text{rb}}$ such that

$$a(u_h^{\text{rb}}, v_h^{\text{rb}}) = (f, v_h^{\text{rb}})_\Omega \quad \forall v_h^{\text{rb}} \in V_h^{\text{rb}}.$$

By looking at rbVEM as a standard Galerkin approximation in V_h^{rb} , we can avoid dealing with the consistency error that arises from the non conformity that naturally arises in the virtual element framework.

We observe that continuity and coercivity of the bilinear form a , together with the linearity of the right hand side, ensure the well-posedness of Problem 8, as stated by the Lax–Milgram theorem. The discrete solution operator $T_h : H^1(\Omega) \rightarrow V_h^{\text{rb}} \subset H^1(\Omega)$ is thus defined as $T_h f = u_h^{\text{rb}}$, with u_h^{rb} being the unique solution to Problem 8. In other words, we have

$$a(T_h f, v_h^{\text{rb}}) = (f, v_h^{\text{rb}})_\Omega \quad \forall v_h^{\text{rb}} \in V_h^{\text{rb}}.$$

It holds that the eigenpairs of Problem 6 and T_h are related as in the continuous case. In addition, the operator T_h is compact since its range is a finite dimensional space.

As a consequence, we resort to the theory for spectral approximation of compact operators [16, 4] to carry out the error analysis for our numerical method. Nevertheless, in the context of eigenvalue problems, the mere convergence of the numerical method is not enough to guarantee a correct approximation of the spectrum. Indeed, besides convergence of the discrete eigenpairs, the *correct spectral approximation* requires that no spurious eigenvalues pollute the spectrum, i.e.

- each discrete eigenvalue converges to a continuous one (preserving the ordering);
- each continuous eigenvalue with multiplicity m is approximated by exactly m discrete eigenvalues, counted with their multiplicity.

It is well known that a sufficient condition for obtaining a correct approximation is the uniform convergence of the sequence T_h to T as $h \rightarrow 0$, namely

$$(36) \quad \|T - T_h\|_{\mathcal{L}(H^1(\Omega))} = \sup_{f \in H^1(\Omega)} \frac{\|(T - T_h)f\|_{1,\Omega}}{\|f\|_{1,\Omega}} \longrightarrow 0 \quad \text{for } h \rightarrow 0.$$

We emphasize that the uniform convergence (36) directly follows from an *a priori* error estimate for the source problem of kind

$$(37) \quad \|u - u_h^{\text{rb}}\|_{1,\Omega} \leq \mathfrak{E}(h) \|f\|_{0,\Omega} \leq \mathfrak{E}(h) \|f\|_{1,\Omega} \quad \text{with } \mathfrak{E}(h) \rightarrow 0 \quad \text{for } h \rightarrow 0,$$

indeed

$$(38) \quad \|T - T_h\|_{\mathcal{L}(H^1(\Omega))} = \sup_{f \in H^1(\Omega)} \frac{\|(T - T_h)f\|_{1,\Omega}}{\|f\|_{1,\Omega}} = \sup_{f \in H^1(\Omega)} \frac{\|u - u_h^{\text{rb}}\|_{1,\Omega}}{\|f\|_{1,\Omega}} \leq \mathfrak{E}(h).$$

In the next section, we prove that (37) holds true.

5. ERROR ANALYSIS

We present the error estimate in energy norm for the source Problem 8. As we discussed, this ensures the correct spectral approximation of the eigenpairs. We also prove the error estimate in L^2 -norm.

Since the rbVEM approximation of Problem 8 is fully conforming, Galerkin orthogonality and Ceà's lemma hold straightforwardly [22], yielding

$$(39) \quad |u - u_h^{\text{rb}}|_{1,\Omega} \leq C |u - u_I^{\text{rb}}|_{1,\Omega}.$$

We estimate the interpolation error in the following proposition.

Proposition 1. *Let $u \in H^{1+s}(\Omega)$, $1/2 < s \leq 1$, be the unique solution to Problem 7 and $u_I^{\text{rb}} \in V_h^{\text{rb}}$ its interpolant. There exists a constant C , independent of h , such that the following estimate holds*

$$|u - u_I^{\text{rb}}|_{1,\Omega} \leq Ch^s \|f\|_{0,\Omega}.$$

Proof. As usual, we estimate the interpolation error locally in a generic element $E \in \mathcal{T}_h$. Thus, we consider the restriction of u_I^{rb} to E and denote it by $I_E u$. More precisely, the local interpolation operator $I_E : C^0(E) \cap H^1(E) \rightarrow V_h^{\text{rb}}(E) \subset H^1(E)$ is defined as

$$(40) \quad I_E u := \sum_{i=1}^N u(\mathbf{v}_i) \tilde{e}_i^{\text{rb}},$$

where $u(\mathbf{v}_i)$ are the degrees of freedom of u in the discrete space $V_h^{\text{rb}}(E)$, i.e. its values at the vertices of E , and \tilde{e}_i^{rb} are the basis functions of the local space $V_h^{\text{rb}}(E)$.

For $p \in \mathbb{P}_1(E)$ arbitrary we can write

$$(41) \quad |u - I_E u|_{1,E} \leq |u - p|_{1,E} + |p - I_E u|_{1,E}$$

On the other hand, since $I_E p = p$, we estimate the term $|p - I_E u|_{1,E}$ as

$$(42) \quad |p - I_E u|_{1,E} = |I_E p - I_E u|_{1,E} = |I_E(p - u)|_{1,E}.$$

Now we can write

$$(43) \quad |I_E(p - u)|_{1,E} = \left| \sum_{i=1}^N (u(\mathbf{v}_i) - p(\mathbf{v}_i)) \tilde{e}_i^{\text{rb}} \right|_{1,E} \leq \left(\sum_{i=1}^N |\tilde{e}_i^{\text{rb}}|_{1,E} \right) \|u - p\|_{\infty,E}.$$

Now, thanks to our shape regularity assumptions and a standard scaling argument, we have that

$$|\tilde{e}_i^{\text{rb}}|_{1,E} \simeq 1.$$

Then, as the shape regularity of the elements implies that N is uniformly bounded, we have

$$(44) \quad |u - I_E u|_{1,E} \leq C \inf_{p \in \mathbb{P}_1(E)} (|u - p|_{1,E} + \|u - p\|_{\infty,E}).$$

We can now take p as the $L^2(B_E)$ projection of an H^s bounded extension of u to the smallest ball B_E circumscribed to E , and by [22, Theorem 3.1.4] we obtain

$$(45) \quad |u - I_E u|_{1,E} \leq Ch^s |u|_{1+s,E}.$$

The global estimate is then obtained by summing on all local contributions. \square

By combining (39) with Proposition 1, we obtain the following optimal error estimate in energy norm.

Theorem 1. Let $u \in H^{1+s}(\Omega)$, $1/2 < s \leq 1$, be the solution to Problem 7 and let $u_h^{\text{rb}} \in V_h^{\text{rb}}$ be the solution to the discrete Problem 8. There exists a positive constant C , independent of h , such that

$$|u - u_h^{\text{rb}}|_{1,\Omega} \leq Ch^s \|f\|_{0,\Omega}.$$

By Poincaré inequality in $H_0^1(\Omega)$, we exploit the equivalence between $\|\cdot\|_{1,\Omega}$ and $|\cdot|_{1,\Omega}$ to get the uniform convergence (36) directly from the a priori error estimate.

In order to complete the error analysis for the source problem, we resort to a standard duality argument for proving the error estimate in L^2 -norm.

Theorem 2. Let $u \in H^{1+s}(\Omega)$, $1/2 < s \leq 1$, be the solution to Problem 7 and let $u_h^{\text{rb}} \in V_h^{\text{rb}}$ be the solution to the discrete Problem 8. There exists a positive constant C , independent of h , such that, letting $\sigma_0 = \pi/\theta_0$ where θ_0 is the maximum of the interior angles of the polygonal domain Ω , for $\epsilon > 0$ arbitrarily small we have

$$\|u - u_h^{\text{rb}}\|_{0,\Omega} \leq Ch^{s+\sigma_0-\epsilon} \|f\|_{0,\Omega}.$$

Proof. Let $\eta \in H^{1+\sigma}(\Omega)$ be the solution to the dual problem

$$(46) \quad a(v, \eta) = (v, u - u_h^{\text{rb}}) \quad \forall v \in H_0^1(\Omega),$$

which satisfies, for all $\sigma = \sigma_0 - \epsilon$ with $0 < \sigma < \sigma_0$ (see [27]),

$$(47) \quad |\eta|_{1+\sigma,\Omega} \leq C\|u - u_h^{\text{rb}}\|_{0,\Omega}.$$

By testing the above equation with $v = u - u_h^{\text{rb}}$ we estimate the error in the L^2 -norm as follows

$$\begin{aligned} \|u - u_h^{\text{rb}}\|_{0,\Omega}^2 &= a(u - u_h^{\text{rb}}, \eta) = a(u - u_h^{\text{rb}}, \eta - \eta_I) \quad (\text{Galerkin orthogonality}) \\ &\leq C|u - u_h^{\text{rb}}|_{1,\Omega}|\eta - \eta_I|_{1,\Omega} \quad (\text{continuity of } a) \\ (48) \quad &\leq Ch^s|u|_{1+s,\Omega}|\eta - \eta_I|_{1,\Omega} \quad (\text{Theorem 1}) \\ &\leq Ch^s\|f\|_{0,\Omega}h^\sigma|\eta|_{1+\sigma,\Omega} \quad (\text{stability and interpolation estimate}) \\ &\leq Ch^{s+\sigma}\|f\|_{0,\Omega}\|u - u_h^{\text{rb}}\|_{0,\Omega}, \quad ((47) \text{ and } 1/2 < s \leq 1) \end{aligned}$$

where $\eta_I \in V_h^{\text{rb}}$ denotes the interpolant of η in the discrete space V_h^{rb} . A division by $\|u - u_h^{\text{rb}}\|_{0,\Omega}$ yields the desired result. \square

Remark 2. We observe that in the case if the domain Ω is convex, we gain an additional power of h in the L^2 -norm estimate with respect to the error in energy norm. On the other hand, if the domain has large interior angles we gain a power $h^{\sigma_0-\epsilon}$, σ_0 depending on the maximum interior angle of the domain.

6. ERROR ESTIMATES FOR EIGENVALUE PROBLEM

We are now ready to present the convergence results for the approximation of the Laplace eigenproblem in rbVEM framework.

By applying the results given by the Babuška–Osborn theory (see [16, Thm. 9.3–9.7] and [4, Thm. 7.1–7.4]), we obtain the error estimates for the approximation of both the eigenvalues and eigenfunctions. To this aim, we recall the definition of gap between two spaces $\mathcal{E} \subset H^\ell(\Omega)$ and $\mathcal{F} \subset H^\ell(\Omega)$ as

$$\hat{\delta}_\ell(\mathcal{E}, \mathcal{F}) = \max\{\delta_\ell(\mathcal{E}, \mathcal{F}), \delta_\ell(\mathcal{F}, \mathcal{E})\},$$

where

$$\delta_\ell(\mathcal{E}, \mathcal{F}) = \sup_{v \in \mathcal{E}, \|v\|_{\ell, \Omega} = 1} \inf_{w \in \mathcal{F}, \|w\|_{\ell, \Omega} = 1} \|v - w\|_{\ell, \Omega}.$$

In our case, we are interested in $\ell = 0, 1$ measuring the gap either in the L^2 - or H^1 -norm.

Theorem 3. *Let λ be an eigenvalue of Problem 1 of multiplicity m and \mathcal{E}_λ be the corresponding eigenspace. Then, there are exactly m discrete eigenvalues of Problem 6 $\lambda_{j(i),h}^{\text{rb}}$ ($i = 1, \dots, m$) tending to λ . Moreover, assuming that all $u \in \mathcal{E}_\lambda$ satisfy $u \in H^{1+s}(\Omega)$ with $1/2 < s \leq 1$, the following inequalities hold true*

$$|\lambda - \lambda_{j(i),h}^{\text{rb}}| \leq Ch^{2s}, \quad \hat{\delta}_1(\mathcal{E}_\lambda, \oplus_i \mathcal{E}_{j(i),h}^{\text{rb}}) \leq Ch^s, \quad \hat{\delta}_0(\mathcal{E}_\lambda, \oplus_i \mathcal{E}_{j(i),h}^{\text{rb}}) \leq Ch^{s+\sigma_0-\epsilon},$$

where $\mathcal{E}_{r,h}^{\text{rb}}$ is the eigenspace spanned by the approximate eigenfunctions $u_{r,h}^{\text{rb}}$.

Theorem 3 gives us an approximation result for the eigenvalues and for the eigenfunctions in V_h^{rb} . If we interpret Problem 6 as a non conforming discretization of Problem 1 in the global VEM space V_h , the eigenfunctions will be reconstructed using the basis for V_h rather than the one for V_h^{rb} , so that such a theorem will not apply directly. In order to get a convergence estimate we will resort to the following lemma.

Lemma 1. *Let $v_h^{\text{rb}} \in V_h^{\text{rb}}(E)$ and let $v_h \in V_1(E)$ be defined by $v_h = \sum_i v_h^{\text{rb}}(\mathbf{v}_i) e_i$. Then it holds*

$$(49) \quad |v_h^{\text{rb}} - v_h|_{1,E} + h^{-1} \|v_h^{\text{rb}} - v_h\|_{0,E} \leq C \inf_{p \in \mathbb{P}_1(E)} (|v_h^{\text{rb}} - p|_{1,E} + h^{-1} \|v_h^{\text{rb}} - p\|_{0,E})$$

Proof. We observe that, as both $V_1(E)$ and $V_h^{\text{rb}}(E)$ exactly reproduce linears, for all $p \in \mathbb{P}_1(E)$ we have that

$$\sum_i p(\mathbf{v}_i) (e_i - \tilde{e}_i^{\text{rb}}) = 0.$$

Then for $p \in \mathbb{P}_1(E)$ arbitrary we can write

$$(50) \quad \begin{aligned} |v_h^{\text{rb}} - v_h|_{1,E} &= \left| \sum_i v_h^{\text{rb}}(\mathbf{v}_i) (\tilde{e}_i^{\text{rb}} - e_i) \right|_{1,E} \\ &= \left| \sum_i (v_h^{\text{rb}}(\mathbf{v}_i) - p(\mathbf{v}_i)) (\tilde{e}_i^{\text{rb}} - e_i) \right|_{1,E} \\ &\leq \|v_h^{\text{rb}} - p\|_{\infty, \partial E} \sum_i (|\tilde{e}_i^{\text{rb}}|_{1,E} + |e_i|_{1,E}) \leq C \|v_h^{\text{rb}} - p\|_{\infty, \partial E}. \end{aligned}$$

By a standard scaling argument, as $v_h^{\text{rb}} - p$ is a piecewise linear function on ∂E we obtain

$$(51) \quad |v_h^{\text{rb}} - v_h|_{1,E} \leq C \left(|v_h^{\text{rb}} - p|_{1/2, \partial E} + h^{-1/2} \|v_h^{\text{rb}} - p\|_{0, \partial E} \right).$$

By a standard trace theorem we then have

$$(52) \quad \begin{aligned} |v_h^{\text{rb}} - v_h|_{1,E} &\leq C \left(|v_h^{\text{rb}} - p|_{1,E} + h^{-1/2} \|v_h^{\text{rb}} - p\|_{0,E}^{1/2} |v_h^{\text{rb}} - p|_{1,E}^{1/2} \right) \\ &\leq C (|v_h^{\text{rb}} - p|_{1,E} + h^{-1} \|v_h^{\text{rb}} - p\|_{0,E}). \end{aligned}$$

By the arbitrariness of p we get the desired result. \square

Combining Theorem 3 with Lemma 1 we obtain the following corollary

Corollary 1. *Under the assumptions of Theorem 3, letting $\mathcal{E}_{r,h} \subset V_h$ be the eigenspace spanned by the approximate eigenfunctions $u_{r,h}$ of Problem 6(b), we have that*

$$\hat{\delta}_1(\mathcal{E}_\lambda, \oplus_i \mathcal{E}_{j(i),h}) \leq Ch^t, \quad \hat{\delta}_0(\mathcal{E}_\lambda, \oplus_i \mathcal{E}_{j(i),h}) \leq Ch^{t+s},$$

Proof. Let $u_h \in V_h$ and $u_h^{\text{rb}} \in V_h^{\text{rb}}$ be such that for all nodes \mathbf{v} of the mesh \mathcal{T}_h we have $u_h(\mathbf{v}) = u_h^{\text{rb}}(\mathbf{v})$ and such that u_h and u_h^{rb} are, respectively, functions in the eigespaces $\mathcal{E}_{j(i),h}$ and $\mathcal{E}_{j(i),h}^{\text{rb}}$. By Theorem 3, there exists a $u \in \mathcal{E}_\lambda$ with $u \in H^{s+1}(\Omega)$ such that

$$|u - u_h^{\text{rb}}|_{1,\Omega} + h^{-\sigma_0+\varepsilon} \|u - u_h^{\text{rb}}\|_{0,\Omega} \leq Ch^s.$$

Now, letting Π_E^0 denote the $L^2(E)$ projection onto $\mathbb{P}_1(E)$, we can write

$$\begin{aligned} \|u_h^{\text{rb}} - u_h\|_{0,E} &\leq |u_h^{\text{rb}} - u_h|_{1,E} + h^{-1} \|u_h^{\text{rb}} - u_h\|_{0,E} \\ &\leq |u_h^{\text{rb}} - \Pi_E^0 u - \int_E (u_h^{\text{rb}} - u)|_{1,E} + h^{-1} \|u_h^{\text{rb}} - \Pi_E^0 u - \int_E (u_h^{\text{rb}} - u)\|_{0,E} \\ &\leq |u_h^{\text{rb}} - u|_{1,E} + h^{-1} \|u_h^{\text{rb}} - u - \int_E (u_h^{\text{rb}} - u)\|_{0,E} + |u - \Pi_E^0 u|_{1,E} + h^{-1} \|u - \Pi_E^0 u\|_{0,\Omega} \\ &\leq C (|u_h^{\text{rb}} - u|_{1,E} + |u - \Pi_E^0 u|_{1,E} + h^{-1} \|u - \Pi_E^0 u\|_{0,E}). \end{aligned}$$

Theorem 3 combined with standard piecewise polynomial approximation results immediately yield

$$\delta_1(\oplus_i \mathcal{E}_{j(i),h}, \mathcal{E}_\lambda) \leq Ch^s, \quad \delta_0(\oplus_i \mathcal{E}_{j(i),h}, \mathcal{E}_\lambda) \leq Ch^{s+\sigma_0-\varepsilon}.$$

Analogously, one can prove that

$$\delta_1(\mathcal{E}_\lambda, \oplus_i \mathcal{E}_{j(i),h}) \leq Ch^s, \quad \delta_0(\mathcal{E}_\lambda, \oplus_i \mathcal{E}_{j(i),h}) \leq Ch^{s+\sigma_0-\varepsilon},$$

which concludes the proof. \square

7. NUMERICAL TESTS

In this section we present a wide set of numerical tests confirming our theoretical findings. We first consider the Laplace eigenproblem on the unit square. We investigate the robustness of the rbVEM with respect to the number M of reduced basis functions employed to construct the discrete space. Then, we compare the approximation properties of our novel rbVEM scheme with those of standard VEM and the alternative rbstab-VEM discussed in Remark 1. We further test the optimality of our method in the case of singular eigenfunctions by considering the L-shaped domain benchmark test and, finally, we solve a second order problem with piecewise constant coefficient.

We point out that the discrete space $V_h^{\text{rb}}(E)$ for a generic mesh element E with N vertices is constructed by means of the reduced basis functions computed once and for all as described in [23, Sect. 6].

7.1. Laplace eigenproblem on the unit square. In order to have at disposal the eigenpairs in analytical form, we solve the Laplace eigenvalue problem in the unit square. In this case, the exact eigenvalues are given by $(i^2 + j^2)\pi^2$ with $i, j \in \mathbb{N} \setminus \{0\}$ with eigenfunctions $\sin(i\pi x)\sin(j\pi y)$.

As we discussed in Section 3, the definition of the new discrete space V_h^{rb} depends on the number M of reduced basis functions used to approximate the virtual basis functions, see (26) and 27. On the other hand, we point out that the number M is fixed *a priori*. The careful reader may wonder whether the computed eigenvalues depend on this parameter M . In order to investigate this aspect, we solve Problem 6 with different discrete spaces V_h^{rb} for several choices of

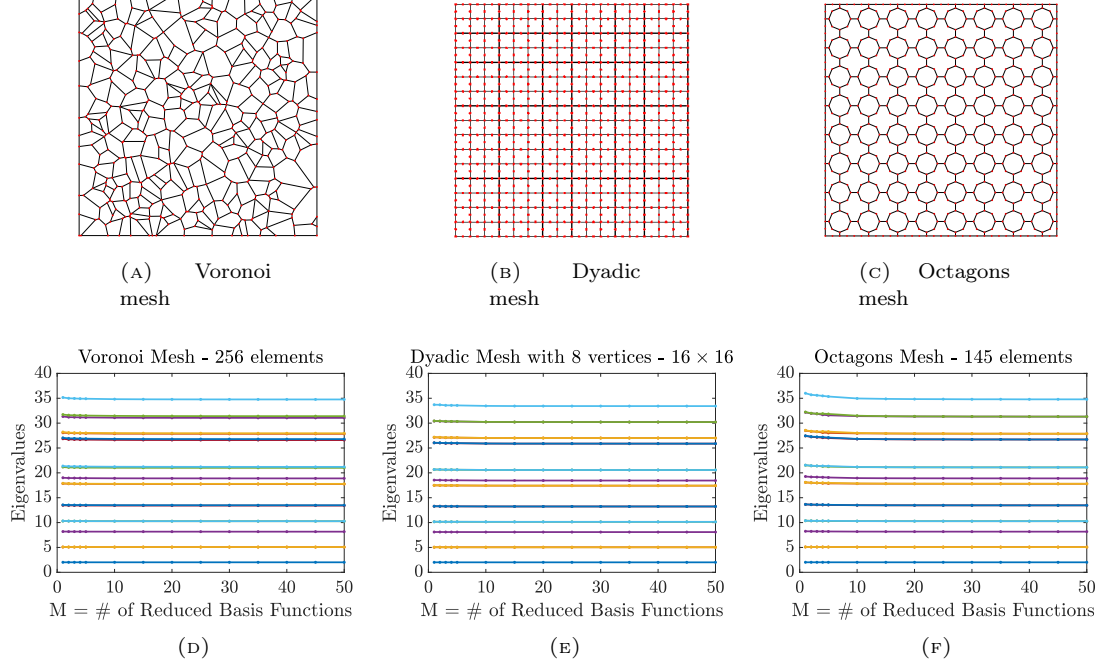


FIGURE 3. The robustness of rbVEM with respect to the number of reduced basis functions M . In the top line we depict the three different considered meshes, whereas in the bottom line we plot the computed eigenvalues.

M , varying from 1 to 50. We also consider three different meshes: Voronoi, dyadic (i.e. squares with an additional dofs at each edge middle point), and octagons, as depicted in Figure 3. In the same figure, we also plot the discrete eigenvalues rescaled by a factor π^2 with respect to M . It is evident that the computed eigenvalues lie on horizontal lines, meaning that our method is robust since the eigenvalues are independent of M . For this reason, in the following numerical tests, we construct the space V_h^{rb} with $M = 1$.

We now compare the approximation properties of our rbVEM and rb-stab-VEM formulations with respect to those of the stabilized VEM on a sequence of Voronoi meshes. Concerning the VEM stabilization parameters, we consider two cases: a fully stabilized formulation with $\alpha = 0.35$, $\beta = 1$ and a partially stabilized formulation with $\alpha = 0.35$ and $\beta = 0$, in the spirit of [19]. The results are reported in Figure 4, where each line refers to the employed numerical method, namely VEM ($\alpha = 0.35$, $\beta = 1$), VEM ($\alpha = 0.35$, $\beta = 0$), rbVEM and rb-stab-VEM ($\chi = 0, 1$), respectively. In the first column we plot the first 20 discrete and exact eigenvalues, in the second column we plot the error for the first 220 eigenvalues with respect to their index and, finally, in the third column we plot the error convergence for the first 10 eigenvalues when refining h . We observe that the standard VEM with $\beta = 0$ and our rbVEM and rb-stab-VEM behave equivalently, showing a significant improvement with respect to standard VEM with $\beta = 1$. We also point out that the convergence rate of the error is two as predicted by the theoretical results (see Theorem 3). Moreover, by

Eigenvalues on Voronoi Meshes - VEM $\alpha = 0.35, \beta = 1$

Index of Eigenvalue	1	2	3	4	5					
256 Elements	2.0031	3.4950	4.0009	4.9486	4.9883	...				
Index of Eigenvalue	8	9	10	11	12	13	14	15		
1024 Elements	...	13.0276	16.8463	16.9775	17.0105	17.7225	17.9448	18.0133	18.0961	...
Index of Eigenvalue	30	31	32	33	34	35	36	37		
4096 Elements	...	45.0668	49.9084	50.0284	50.0628	50.2086	51.4368	51.9794	52.0531	...

TABLE 1. Eigenvalues computed with Stabilized VEM on Voronoi meshes. Spurious eigenvalues are reported into boxes.

comparing the error plots in the second column, we notice that the discrete methods based on the reduced basis approach approximate well a larger portion of the spectrum since less oscillations occur. In addition, the fully stabilized VEM ($\alpha = 0.35, \beta = 1$) produces spurious eigenvalues, as reported in Table 1, where spurious modes are displayed into boxes.

As discussed in Section 2, the term $b(\Pi^0 u_h, \Pi^0 v_h)$ may have a kernel, and this is the interesting case when considering VEM ($\beta = 0$) or rb-stab-VEM ($\chi = 0$) in the spirit of [19]. Nevertheless, on the sequence of Voronoi meshes we considered for our tests, the non-stabilized mass term has full rank. Thus, we repeat the same comparison on a sequence of dyadic meshes, giving, for $\beta, \chi = 0$, singular mass matrices. In this test, the stability parameters for standard VEM are set to $\alpha = \beta = 1$. The associated results are collected in Figure 5: we observe the same behavior as for the Voronoi case, so that we can draw the same conclusions.

7.2. Laplace eigenproblem on the L-shaped domain. We consider the benchmark test proposed in [24]. In this case, we solve the Laplace eigenproblem with homogeneous Neumann boundary conditions on the L-shaped domain $\Omega = (-1, 1)^2 \setminus \Omega_0$, with $\Omega_0 = (0, 1) \times (-1, 0)$, which is depicted in Figure 6. Since an analytical expression for the exact eigenvalues is not available, our reference solutions are the first five eigenvalues computed on a very fine triangulation as given in [24], i.e.

$$\begin{aligned}\lambda_1 &= 0.147562182408 \text{E+01} \\ \lambda_2 &= 0.353403136678 \text{E+01} \\ \lambda_3 &= 0.986960440109 \text{E+01} \\ \lambda_4 &= 0.986960440109 \text{E+01} \\ \lambda_5 &= 0.113894793979 \text{E+02}.\end{aligned}$$

It is well-known that the eigenfunction u_1 associated with λ_1 is singular due to the re-entrant corner so that $u_1 \in H^{1+s}(\Omega)$ for all $s < 2/3$. Consequently, we expect a convergence rate of $4/3$. We point out that the eigenfunctions associated with $\lambda_2, \dots, \lambda_5$ are smooth, therefore the expected convergence rate of such eigenvalues is 2.

We report the convergence plots in Figure 7. More precisely, we analyze once again the stabilized VEM ($\alpha = \beta = 1$), the partially stabilized VEM ($\alpha = 1, \beta = 0$), the novel rbVEM and the rb-stab-VEM ($\chi = 0, 1$). The four methods share the same convergence history; in particular, the rbVEM and the rb-stab-VEM are optimal even for singular eigenfunctions.

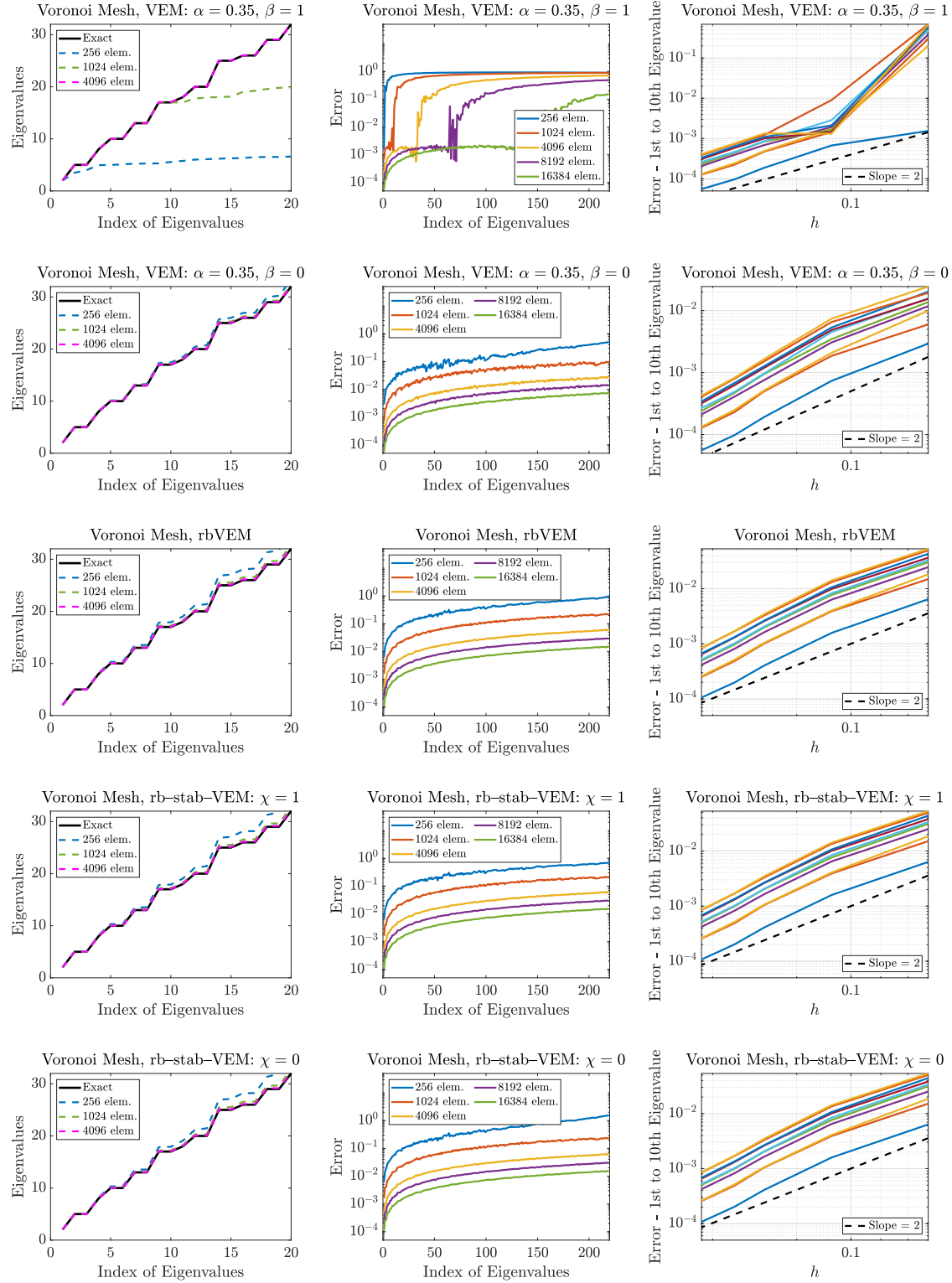


FIGURE 4. Comparison between VEM (first and second line) rbVEM (third line) and rb-stab-VEM (fourth and fifth line) on a sequence of Voronoi meshes. First column: plots of the first 20 computed and exact eigenvalues. Second column: error plots for the first 220 eigenvalues with respect to their index. Third column: error plots for the first 10 eigenvalues when refining the mesh size.

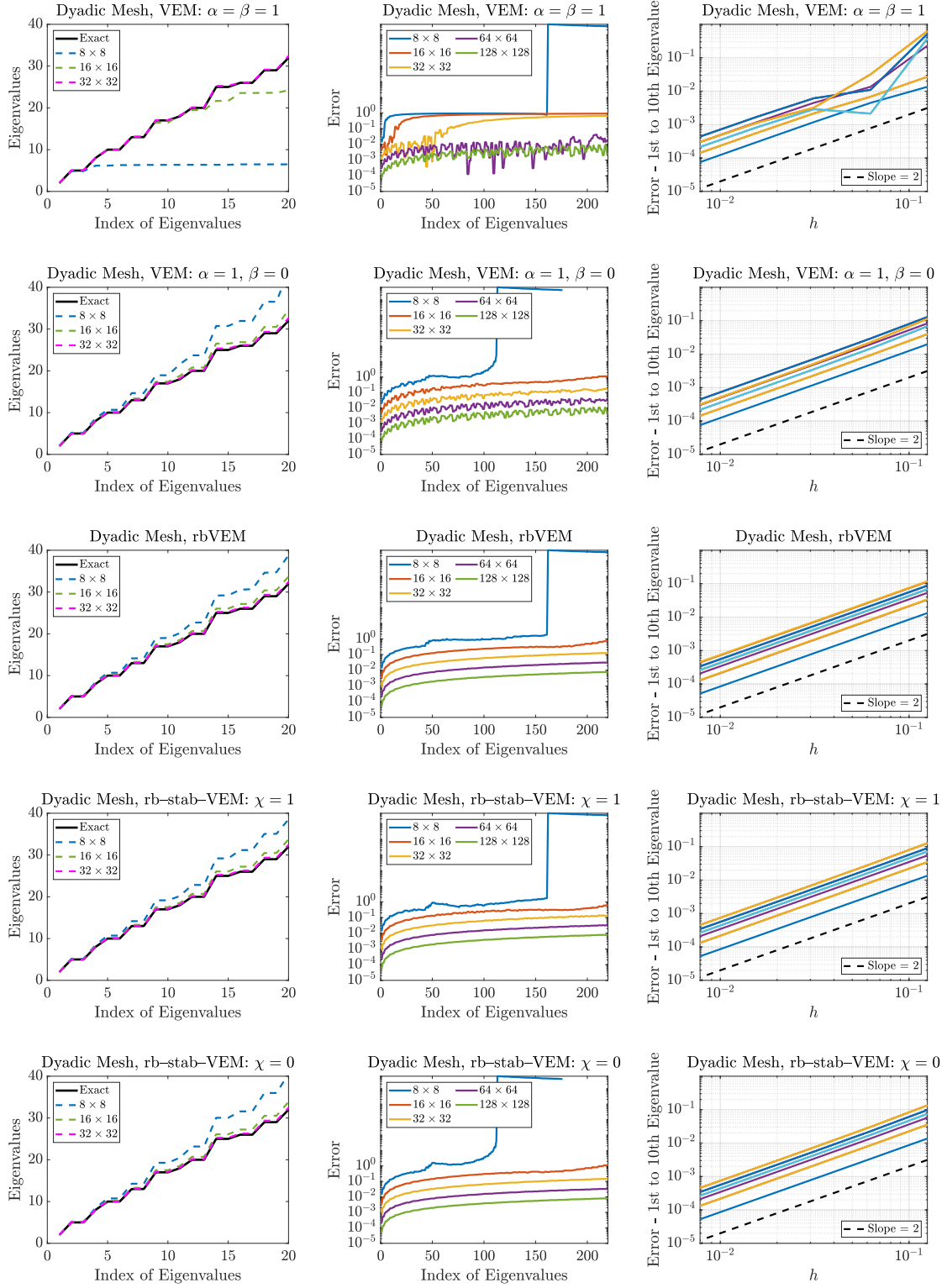


FIGURE 5. Comparison between VEM (first and second line) rbVEM (third line) and rb-stab-VEM (fourth and fifth line) on a sequence of dyadic meshes. First column: plots of the first 20 computed and exact eigenvalues. Second column: error plots for the first 220 eigenvalues with respect to their index. Third column: error plots for the first 10 eigenvalues when refining the mesh size.

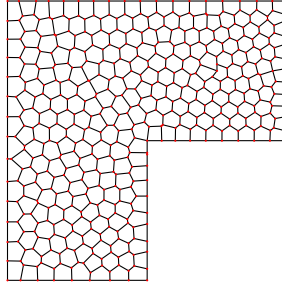


FIGURE 6. A Voronoi mesh for the L-shaped domain $\Omega = (-1, 1)^2 \setminus \Omega_0$ with $\Omega_0 = (0, 1) \times (-1, 0)$.

7.3. Second order problem with piecewise constant coefficient. We consider another benchmark test from [24]: we seek for the eigenvalues of a second order problem with piecewise constant diffusivity \mathcal{K} and homogeneous Neumann boundary conditions. The continuous bilinear form a takes now the form

$$a(u, v) = (\mathcal{K}\nabla u, \nabla v)_\Omega.$$

The discrete bilinear form a_h within the stabilized VEM setting is defined analogously to (11), see [5]. On the other hand, all quantities are computed exactly in the case of rbVEM.

Let $\Omega = (-1, 1)^2$ be decomposed into two regions Ω_1 and Ω_δ with diffusivity $\mathcal{K} = \text{Id}$ and $\mathcal{K} = \delta \text{Id}$, respectively, as depicted in Figure 8. We discretize the domain by a family of Voronoi meshes and we consider four different values of δ , namely $\delta = 2, 10, 100, 10^8$. We then compute the first two eigenvalues, whose reference solution computed on a very fine triangulation with high order finite elements is given by [24]

$$\begin{array}{ll} \delta = 2 : & \delta = 10 : \\ \lambda_1 = 0.3317548763415 \text{ E+01}, & \lambda_1 = 0.4533851871670 \text{ E+01}, \\ \lambda_2 = 0.3366324157260 \text{ E+01}, & \lambda_2 = 0.6250332186603 \text{ E+01}, \\ \\ \delta = 100 : & \delta = 10^8 : \\ \lambda_1 = 0.4893193324891 \text{ E+01}, & \lambda_1 = 0.4934802158785 \text{ E+01}, \\ \lambda_2 = 0.7206675422492 \text{ E+01}, & \lambda_2 = 0.7225211232692 \text{ E+01}. \end{array}$$

Convergence plots of the first eigenvalue are reported in Figure 9, whereas those of the second eigenvalue are in Figure 10. More precisely, we compare rbVEM with the stabilized VEM ($\alpha = 0.25, 0.5, 1, \beta = 1$) and the rb-stab-VEM ($\chi = 1$). We observe that rbVEM, rb-stab-VEM and VEM ($\alpha = \beta = 1$) share the same optimal convergence history: all eigenvalues converge with rate two, except for the second one in correspondence of $\delta = 10$, whose error decays with order 0.84, as already shown in [26]. On the other hand, the stabilized VEM with $\alpha = 0.25$ and $\alpha = 0.5$ presents some oscillations, especially for the second eigenvalue in correspondence of $\delta = 2, 10$. We finally point out that VEM and rb-stab-VEM have been also tested for $\beta = 0$ and $\chi = 0$, respectively: as in the previous test cases, the methods showed optimal rates of convergence and have not been plotted for the sake of readability.

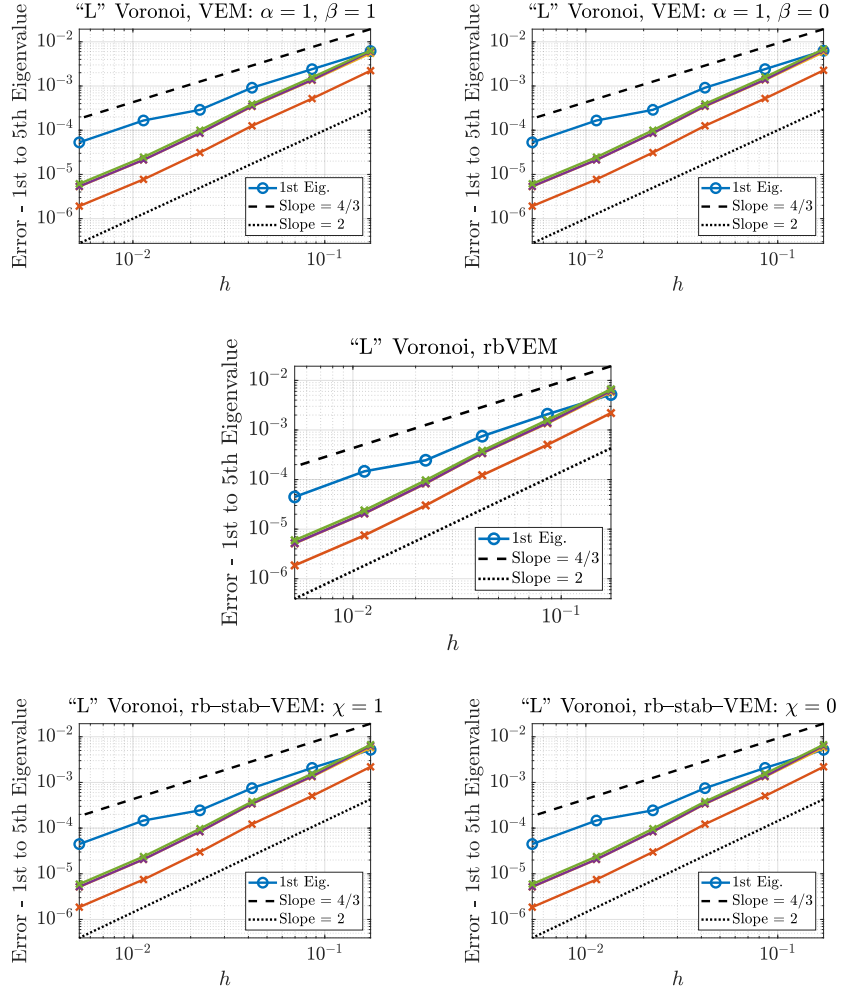


FIGURE 7. Convergence of eigenvalues with respect to h on a sequence of Voronoi meshes for the L-shaped domain: VEM (first line), rbVEM (second line) and rb-stab-VEM (third line).

8. CONCLUSION

We introduced the stabilization free rbVEM for the approximation of eigenvalue problems. The presence of stabilization parameters in standard VEM formulations may produce spurious eigenmodes. In order to avoid the parameters dependence, we employed the reduced basis method to efficiently solve the elemental equations defining the virtual basis functions. Thus, we were able to design a new fully conforming discrete space based on the original VEM.

We proved that the rbVEM discretization of the Poisson problem is optimal in both H^1 - and L^2 -norms. Moreover, we established the correct spectral approximation of the Laplace eigenvalue

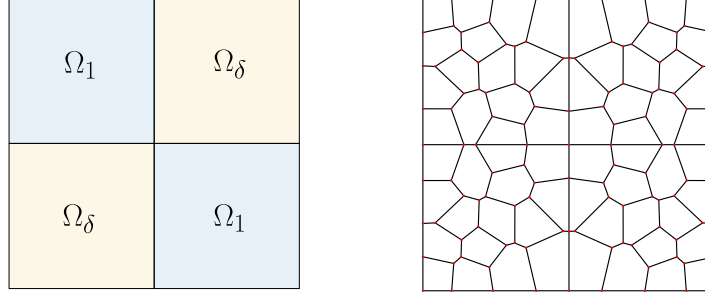


FIGURE 8. Subdivision of Ω into subdomains with different diffusivity and example of Voronoi mesh.

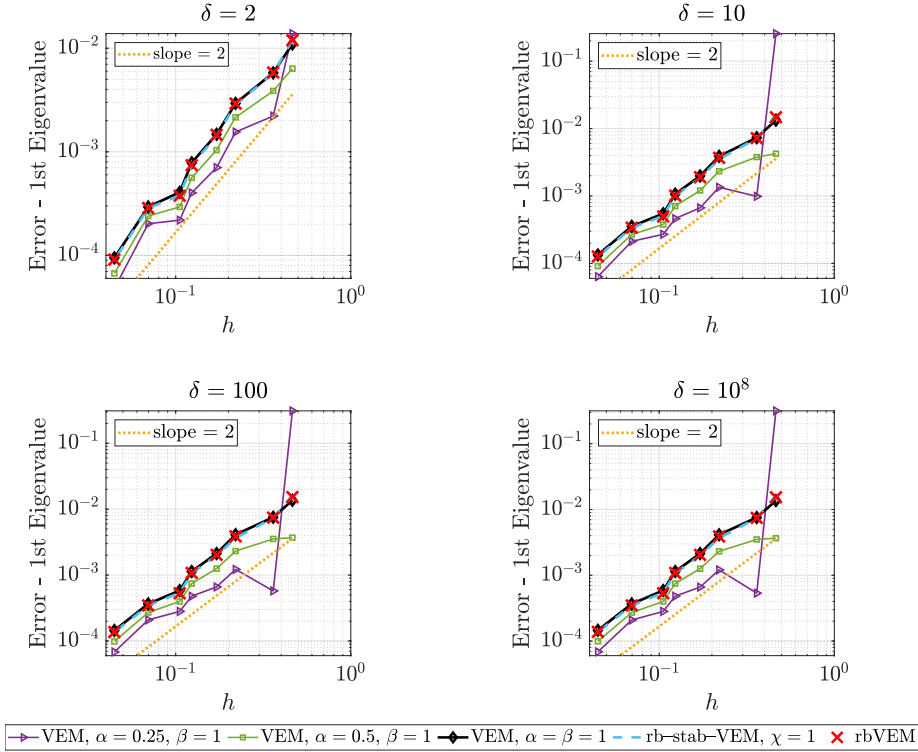


FIGURE 9. Convergence of the first eigenvalue for different values of diffusivity

problem, with optimal convergence rate of the eigenfunctions and the usual doubled rate for the eigenvalues. A wide range of numerical tests confirmed our theoretical findings.

In our tests we also studied the behavior of alternative formulations *à la* VEM, i.e. the rb-stab-VEM, where the reduced basis technique is employed to design the stability terms. This scheme performed equivalently to our rbVEM, which is covered by the theory. This behavior was expected

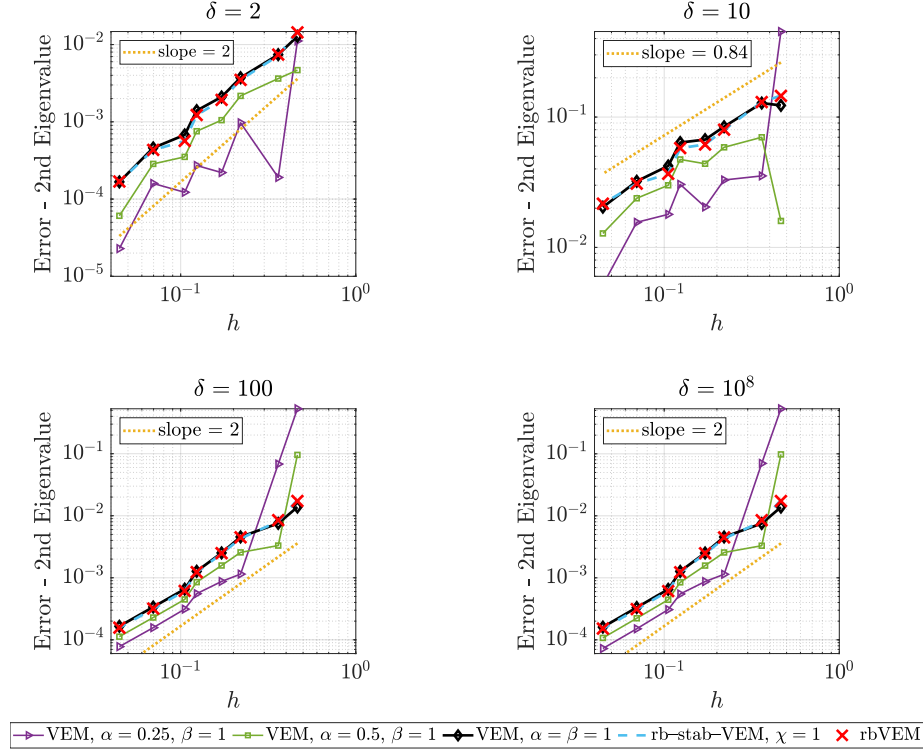


FIGURE 10. Convergence of the second eigenvalue for different values of diffusivity

since in virtual elements approximations the stability term is only required to scale as the actual non-computable term and not to fulfill good approximation properties.

9. ACKNOWLEDGMENTS

The authors are members of GNCS–INdAM Research Group and are grateful to Daniele Prada (IMATI–CNR Pavia) for providing the mesh files employed for the numerical tests.

S. Bertoluzza is partially supported by MUR–PRIN/PNRR Bando 2022 (grant P2022BH5CB).

F. Gardini is partially supported by the National Recovery and Resilience Plan, Mission 4 Component 2 - Investment 1.4 - National Center for HPC, Big Data and Quantum Computing, spoke 6.

APPENDIX A. REDUCED BASIS METHOD IN SUPPORT OF VEM

A.1. Computing the basis functions. In this appendix we recall the main features of the reduced basis approach we designed in [23] for efficiently solving the parametric Problem 5. The efficiency of the method relies on the *affine decomposition* property. Indeed, from (20), we can write

$$(53) \quad \mathcal{A}(\hat{w}, \hat{v}; E) = \sum_{i=1}^N \mathcal{A}(\hat{w}, \hat{v}; T_i) \quad \text{with} \quad \mathcal{A}(\hat{w}, \hat{v}; T_i) = \left(|\det(\mathsf{L}_{E,i}^{-1})| \mathsf{L}_{E,i}^\top \mathsf{L}_{E,i} \nabla \hat{w}, \nabla \hat{v} \right)_{\hat{T}_i}.$$

Since the matrix $|\det(\mathbf{L}_{E,i}^{-1})| \mathbf{L}_{E,i}^\top \mathbf{L}_{E,i}$ is symmetric, we can rewrite it in terms of a basis $\mathcal{S}^1, \mathcal{S}^2, \mathcal{S}^3$ for the space of 2×2 symmetric matrices, i.e.

$$(54) \quad \det(\mathbf{L}_{E,i}^{-1}) | \mathbf{L}_{E,i}^\top \mathbf{L}_{E,i} = \sum_{\nu=1}^3 c_i^\nu [E] \mathcal{S}^\nu.$$

Hence we find the decomposition

$$(55) \quad \mathcal{A}(\hat{w}, \hat{v}; E) = \sum_{i=1}^N \sum_{\nu=1}^3 c_i^\nu [E] \mathcal{A}^{i,\nu}(\hat{w}, \hat{v}) \quad \text{with} \quad \mathcal{A}^{i,\nu}(\hat{w}, \hat{v}) = (\mathcal{S}^\nu \nabla \hat{w}, \nabla \hat{v})_{\hat{T}_i},$$

where only the coefficients $c_i^\nu [E]$ depend on the parameter, whereas the form $\mathcal{A}^{i,\nu}$ depends only on \hat{w} and \hat{v} . Such decomposition is fundamental for the design of an efficient method. Indeed, once the reduced basis space is constructed, the building blocks $\mathcal{A}^{i,\nu}$ are computed and stored. Thus, for each instance of the parameter, the bilinear form \mathcal{A} is easily computed exploiting the pre-computed objects. The same decomposition holds for the right hand side of Problem 5, we have

$$(56) \quad \mathcal{A}(\hat{\Theta}_j, \hat{v}; E) = \sum_{i=1}^N \sum_{\nu=1}^3 c_i^\nu [E] \mathcal{F}_j^{i,\nu}(\hat{v}) \quad \text{with} \quad \mathcal{F}_j^{i,\nu}(\hat{v}) = (\mathcal{S}^\nu \nabla \hat{\Theta}_j, \nabla \hat{v})_{\hat{T}_i}.$$

In order to construct our reduced basis space, we solve Problem 5 for a sufficiently large sample of polygons $E_\ell \in \mathcal{P}$, for $\ell = 1, \dots, L$. We thus obtain a collection of snapshots $\hat{d}_{i,\delta}^{\text{rb}}[E_\ell]$ defined on the fine mesh \mathcal{T}_δ . The application of the Proper Orthogonal Decomposition (see [23, Sect. 5.1] for more details) yields the construction of the reduced space, spanned by the functions $\hat{\xi}_1^\ell, \dots, \hat{\xi}_N^\ell$ for $\ell = 1, \dots, L$, which are linear combinations of $\hat{d}_{i,\delta}^{\text{rb}}[E_\ell]$. At this stage, by exploiting the affine decomposition, we can pre-compute and store $\mathcal{A}^{i,\nu}$ and $\mathcal{F}_j^{i,\nu}$, so that we have

$$(57) \quad \mathbf{A}_i^\nu(j, j', \ell, \ell') = \mathcal{A}^{i,\nu}(\hat{\xi}_j^\ell, \hat{\xi}_{j'}^{\ell'}), \quad \mathbf{F}_i^\nu(j, j', \ell) = \mathcal{F}_j^{i,\nu}(\hat{\xi}_j^\ell)$$

for $\ell, \ell' = 1, \dots, M$, $j, j' = 1, \dots, N$, and $\nu = 1, 2, 3$. We point out that $M \leq L$ denotes the dimension (i.e. the accuracy) of the reduced basis space.

For each new polygon E with N vertices, we solve Problem 5 in the reduced space. We thus obtain $\hat{d}_{i,\delta}^{\text{rb}}[E]$ in (23) as the linear combination

$$(58) \quad \hat{d}_{i,\delta}^{\text{rb}}[E] = \sum_{\ell=1}^M \mathbf{x}_\ell^{E,j} \hat{\xi}_j^\ell,$$

where the coefficients $\mathbf{x}_\ell^{E,j}$ are solution of the $M \times M$ linear system

$$(59) \quad \mathbf{A}[E] \mathbf{x}^{E,j} = \mathbf{F}[E],$$

which is efficiently assembled by means of the affine decomposition bricks (57), pre-computed only once at offline stage. Moreover, if M is small, then the above system is also cheaply solved. We finally obtain the functions $e_{M,i}^{\text{rb}}[E]$ in (24) as

$$(60) \quad e_{M,i}^{\text{rb}}[E] = \hat{e}_{M,i}^{\text{rb}}[E] \circ \mathcal{L}_E \quad \text{where} \quad \hat{e}_{M,i}^{\text{rb}}[E] = \hat{\Theta}_i + \hat{d}_{i,\delta}^{\text{rb}}[E].$$

A.2. Computing the matrices in the rbVEM space. We now briefly describe how the idea underlying the reduced basis method can be exploited to cheaply compute the stiffness and mass matrices in the space $V_h^{\text{rb}}(E) = \mathbb{P}_1(E) \oplus W_h^{\text{rb}}(E)$. We highlight that the polynomial contribution is computed as in standard virtual element framework, while the contribution in $W_h^{\text{rb}}(E)$ is computed using the affine decomposition. The entire procedure is summarized in Algorithm 1.

The construction of $V_h^{\text{rb}}(E)$ as the direct sum of two spaces implies that the stiffness matrix \mathbf{K} can be decomposed as

$$(61) \quad \mathbf{K} = \Pi^{\nabla} + \mathbf{K}^{\text{rb}}.$$

The matrix $\Pi_{i,j}^{\nabla} = a^E(\Pi^{\nabla} e_i, \Pi^{\nabla} e_j)$ is computed by projecting the basis functions e_1, \dots, e_N of the standard VEM space $V_1(E)$ through the operator Π^{∇} defined in (3) (see [9]). The term \mathbf{K}^{rb} is related to the virtual part of $V_1(E)$ which is not computable through the degrees of freedom. On the other hand, such contribution turns out to be fully computable in $W_h^{\text{rb}}(E)$. Thus, we can write

$$(62) \quad \mathbf{K}^{\text{rb}} = (\mathbf{Id}(N) - \Pi^{\nabla})^{\top} \Psi (\mathbf{Id}(N) - \Pi^{\nabla}),$$

where $\mathbf{Id}(N)$ is the $N \times N$ identity matrix and $\Psi_{i,j} = a^E(e_{M,i}^{\text{rb}}[E], e_{M,j}^{\text{rb}}[E])$.

We now describe how to cheaply compute $a^E(e_{M,i}^{\text{rb}}[E], e_{M,j}^{\text{rb}}[E])$. Let us denote by \widehat{a}^E the bilinear form on the reference element \widehat{E} obtained by change of variable in a^E , that is

$$(63) \quad \widehat{a}^E(w, v) = \sum_{i=1}^N \left(|\det(\mathbf{L}_{E,i}^{-1})| \mathbf{L}_{E,i}^{\top} \mathcal{K} \mathbf{L}_{E,i} \nabla \widehat{w}, \nabla \widehat{v} \right)_{\widehat{T}_i},$$

hence the following identity holds

$$(64) \quad a^E(e_{M,i}^{\text{rb}}[E], e_{M,j}^{\text{rb}}[E]) = \widehat{a}^E(\widehat{e}_{M,i}^{\text{rb}}[E], \widehat{e}_{M,j}^{\text{rb}}[E]).$$

It is clear that all computations can be thus carried out in the reference element. Indeed, by using (60), we find the expansion

$$a^E(e_{M,i}^{\text{rb}}[E], e_{M,j}^{\text{rb}}[E]) = \widehat{a}^E(\widehat{\Theta}_i, \widehat{\Theta}_j) + \sum_{\ell=1}^M \mathbf{x}_{\ell}^{E,j} \widehat{a}^E(\widehat{\xi}_i^{\ell}, \widehat{\Theta}_j) + \sum_{\ell=1}^M \mathbf{x}_{\ell}^{E,j} \widehat{a}^E(\widehat{\Theta}_i, \widehat{\xi}_j^{\ell}) + \sum_{\ell, \ell'=1}^M \mathbf{x}_{\ell}^{E,j} \widehat{a}^E(\widehat{\xi}_i^{\ell'}, \widehat{\xi}_j^{\ell}),$$

where the bricks $\widehat{a}^E(\widehat{\xi}_i^{\ell'}, \widehat{\xi}_j^{\ell})$ are computed by affine decomposition as

$$(65) \quad \widehat{a}^E(\widehat{\xi}_i^{\ell'}, \widehat{\xi}_j^{\ell}) = \sum_{i=1}^N \sum_{\nu=1}^4 c_i^{\nu}[E] \mathbf{A}_i^{\nu}(j, j', \ell, \ell')$$

and an additional element \mathcal{S}^4 is added to $\mathcal{S}^1, \mathcal{S}^2, \mathcal{S}^3$ for dealing with the non-symmetric 2×2 matrix $\det(\mathbf{L}_{E,i}^{-1}) \mathbf{L}_{E,i}^{\top} \mathcal{K} \mathbf{L}_{E,i}$ as [23, Sect. 7]

$$(66) \quad \det(\mathbf{L}_{E,i}^{-1}) \mathbf{L}_{E,i}^{\top} \mathcal{K} \mathbf{L}_{E,i} = \sum_{\nu=1}^4 c_i^{\nu}[E] \mathcal{S}^{\nu}.$$

The same reasoning applies for the construction of the mass matrix \mathbf{M} in $V_h^{\text{rb}}(E)$. As already mentioned when constructing Problem 6 in $V_h^{\text{rb}}(E)$, here cross terms are nonzero, thus we have

$$(67) \quad \mathbf{M} = \mathbf{M}^{\nabla} + \mathbf{M}^{\text{rb}} + \mathbf{M}^{\nabla, \text{rb}} + (\mathbf{M}^{\nabla, \text{rb}})^{\top}.$$

The term \mathbf{M}^∇ is the mass matrix of the polynomial part, i.e. $\mathbf{M}_{i,j}^\nabla = b^E(\Pi^\nabla e_i, \Pi^\nabla e_j)$. The second term is the mass matrix in the space $W_h^{\text{rb}}(E)$ and is assembled similarly to \mathbf{K}^{rb} as

$$(68) \quad \mathbf{M}^{\text{rb}} = (\text{Id}(N) - \nabla^\nabla)^\top \Phi (\text{Id}(N) - \nabla^\nabla),$$

where $\Phi_{i,j} = b^E(e_{M,i}^{\text{rb}}[E], e_{M,j}^{\text{rb}}[E])$. As before, we define the bilinear form on the reference element

$$(69) \quad \widehat{b}^E(w, v) = \sum_{i=1}^N \gamma_i[E] (\widehat{w}, \widehat{v})_{\widehat{T}_i} \quad \text{where} \quad \gamma_i[E] = |\det(\mathbf{L}_{E,i}^{-1})|,$$

so that the following relation holds

$$b^E(e_{M,i}^{\text{rb}}[E], e_{M,j}^{\text{rb}}[E]) = \widehat{b}^E(\widehat{\Theta}_i, \widehat{\Theta}_j) + \sum_{\ell=1}^M \times_\ell^{E,j} \widehat{b}^E(\widehat{\xi}_i^\ell, \widehat{\Theta}_j) + \sum_{\ell=1}^M \times_\ell^{E,j} \widehat{b}^E(\widehat{\Theta}_i, \widehat{\xi}_j^\ell) + \sum_{\ell, \ell'=1}^M \times_\ell^{E,j} \widehat{b}^E(\widehat{\xi}_i^\ell, \widehat{\xi}_j^{\ell'}).$$

Therefore, having pre-computed the building blocks $\mathbf{B}_i(j, j', \ell, \ell') = (\widehat{\xi}_j^\ell, \widehat{\xi}_{j'}^{\ell'})_{\widehat{T}_i}$ at offline stage, we easily construct

$$(70) \quad \widehat{b}^E(\widehat{\xi}_j^\ell, \widehat{\xi}_{j'}^{\ell'}) = \sum_{i=1}^N \gamma_i[E] \mathbf{B}_i(j, j', \ell, \ell').$$

Finally, $\mathbf{M}^{\nabla, \text{rb}}$ is built as

$$(71) \quad \mathbf{M}^{\nabla, \text{rb}} = (\text{Id}(N) - \nabla^\nabla)^\top \tilde{\Phi},$$

with $\tilde{\Phi}_{i,j} = b^E(e_{M,i}^{\text{rb}}[E], \Pi^\nabla e_j)$.

REFERENCES

- [1] B. Ahmad, A. Alsaedi, F. Brezzi, L. D. Marini, and A. Russo. Equivalent projectors for virtual element methods. *Computers & Mathematics with Applications*, 66(3):376–391, 2013.
- [2] L. Alzaben, D. Boffi, A. Dedner, and L. Gastaldi. On the stabilization of a virtual element method for an acoustic vibration problem. *Mathematical Models and Methods in Applied Sciences*, 35(03):655–701, 2025.
- [3] P. F. Antonietti, L. Beirão da Veiga, and G. Manzini. *The virtual element method and its applications*, volume 31. Springer, 2022.
- [4] I. Babuška and J. Osborn. Eigenvalue problems. *Handbook of numerical analysis.*, 2:641, 1991.
- [5] L. Beirão da Veiga, F. Brezzi, L. D. Marini, and A. Russo. Virtual element method for general second-order elliptic problems on polygonal meshes. *Mathematical Models and Methods in Applied Sciences*, 26(04):729–750, 2016.
- [6] L. Beirão da Veiga, F. Brezzi, L. D. Marini, and A. Russo. The virtual element method. *Acta Numerica*, 32:123–202, 2023.
- [7] L. Beirão da Veiga, K. Lipnikov, and G. Manzini. *The mimetic finite difference method for elliptic problems*, volume 11. Springer, 2014.
- [8] L. Beirão da Veiga, F. Brezzi, A. Cangiani, G. Manzini, L. D. Marini, and A. Russo. Basic principles of virtual element methods. *Mathematical Models and Methods in Applied Sciences*, 23(01):199–214, 2013.
- [9] L. Beirão da Veiga, F. Brezzi, L. D. Marini, and A. Russo. The hitchhiker’s guide to the virtual element method. *Mathematical models and methods in applied sciences*, 24(08):1541–1573, 2014.
- [10] L. Beirão da Veiga, D. Mora, G. Rivera, and R. Rodríguez. A virtual element method for the acoustic vibration problem. *Numerische Mathematik*, 136(3):725–763, 2017.
- [11] S. Berrone, A. Borio, D. Fassino, and F. Marcon. Stabilization-free Virtual Element Method for 2D second order elliptic equations. *Computer Methods in Applied Mechanics and Engineering*, 438:117839, 2025.
- [12] S. Berrone, A. Borio, and F. Marcon. Comparison of standard and stabilization free virtual elements on anisotropic elliptic problems. *Applied Mathematics Letters*, 129:107971, 2022.
- [13] S. Berrone, A. Borio, and F. Marcon. Lowest order stabilization free virtual element method for the 2d poisson equation. *Computers & Mathematics with Applications*, 177:78–99, 2025.

Algorithm 1 Local assembler for the rbVEM

Data: E , element of \mathcal{T}_h

Compute projectors:

Project basis of $V_1(E)$ onto $\mathbb{P}_1(E)$: $\Pi^\nabla e_j$, for $j = 1, \dots, N$

Build Π^∇ such that $\Pi_{i,j}^\nabla = a^E(\Pi^\nabla e_i, \Pi^\nabla e_j)$

Compute dofs of virtual contribution:

$R = \text{Id}(N) - \Pi^\nabla$, i.e. $R_{i,j} = e_i(\mathbf{v}_j) - \Pi^\nabla e_i(\mathbf{v}_j)$ for $i, j = 1, \dots, N$

Reduced Basis Online Phase:

Given E , compute functions $\hat{e}_{M,j}^{\text{rb}}[E]$ for $j = 1, \dots, N$

by solving reduced system $A[E]x^{E,j} = F[E]$

Stiffness matrix:

Compute affine decomposition coefficients $c_i^\nu[E]$ for $i = 1, \dots, N$, $\nu = 1, 2, 3, 4$

Construct $\hat{a}^E(\hat{\xi}_j^\ell, \hat{\xi}_{j'}^{\ell'}) = \sum_{i=1}^N \sum_{\nu=1}^4 c_i^\nu[E] \mathbf{A}_i^\nu(j, j', \ell, \ell')$ by affine decomposition

Build stiffness Ψ , i.e. $\Psi_{i,j} = a^E(e_{M,i}^{\text{rb}}[E], e_{M,j}^{\text{rb}}[E])$

Compute $K^{\text{rb}} = R^\top \Psi R$

Compute stiffness matrix in rbVEM framework $K = \Pi^\nabla + K^{\text{rb}}$

Mass matrix:

Build M^∇ such that $M_{i,j}^\nabla = b^E(\Pi^\nabla e_i, \Pi^\nabla e_j)$

Compute affine decomposition coefficients $\gamma_i[E]$ for $i = 1, \dots, N$

Construct $\hat{b}^E(\hat{\xi}_j^\ell, \hat{\xi}_{j'}^{\ell'}) = \sum_{i=1}^N \gamma_i[E] \mathbf{B}_i(j, j', \ell, \ell')$ by affine decomposition

Build mass Φ , i.e. $\Phi_{i,j} = b^E(e_{M,i}^{\text{rb}}[E], e_{M,j}^{\text{rb}}[E])$

Compute $M^{\text{rb}} = R^\top \Phi R$

Build cross terms $\tilde{\Phi}$, i.e. $\tilde{\Phi}_{i,j} = b^E(e_{M,i}^{\text{rb}}[E], \Pi^\nabla e_j)$

Compute $M^{\nabla, \text{rb}} = R^\top \tilde{\Phi}$

Compute mass matrix in rbVEM framework $M = M^\nabla + M^{\text{rb}} + M^{\nabla, \text{rb}} + (M^{\nabla, \text{rb}})^\top$

- [14] S. Berrone, M. Pintore, and G. Teora. The lowest-order neural approximated virtual element method on polygonal elements. *Computers & Structures*, 314:107753, 2025.
- [15] S. Bertoluzza, G. Manzini, M. Pennacchio, and D. Prada. Stabilization of the nonconforming virtual element method. *Computers & Mathematics with Applications*, 116:25–47, 2022.
- [16] D. Boffi. Finite element approximation of eigenvalue problems. *Acta numerica*, 19:1–120, 2010.
- [17] D. Boffi, F. Gardini, and L. Gastaldi. Approximation of PDE eigenvalue problems involving parameter dependent matrices. *Calcolo*, 57(4):41, 2020.
- [18] D. Boffi, F. Gardini, and L. Gastaldi. Virtual element approximation of eigenvalue problems. In *The virtual element method and its applications*, pages 275–320. Springer, 2022.
- [19] D. Boffi, F. Gardini, and L. Gastaldi. Virtual element approximation of eigenvalue problems: is the stabilization of the right hand side necessary?. *In preparation*, 2025.
- [20] A. Cangiani, G. Manzini, A. Russo, and N. Sukumar. Hourglass stabilization and the virtual element method. *International Journal for Numerical Methods in Engineering*, 102(3-4):404–436, 2015.
- [21] O. Čertík, F. Gardini, G. Manzini, L. Mascotto, and G. Vacca. The p-and hp-versions of the virtual element method for elliptic eigenvalue problems. *Computers & Mathematics with Applications*, 79(7):2035–2056, 2020.
- [22] P. G. Ciarlet. *The finite element method for elliptic problems*. SIAM, 2002.

- [23] F. Credali, S. Bertoluzza, and D. Prada. Reduced basis stabilization and post-processing for the virtual element method. *Computer Methods in Applied Mechanics and Engineering*, 420:116693, 2024.
- [24] M. Dauge. Benchmark computations for Maxwell equations for the approximation of highly singular solutions. <http://perso.univ-rennes1.fr/monique.dauge/core/index.html>, (accessed on March 10, 2025).
- [25] F. Gardini, G. Manzini, and G. Vacca. The nonconforming virtual element method for eigenvalue problems. *ESAIM: Mathematical Modelling and Numerical Analysis*, 53(3):749–774, 2019.
- [26] F. Gardini and G. Vacca. Virtual element method for second-order elliptic eigenvalue problems. *IMA Journal of Numerical Analysis*, 38(4):2026–2054, 2018.
- [27] P. Grisvard. *Elliptic problems in nonsmooth domains*. SIAM, 2011.
- [28] J. S. Hesthaven, G. Rozza, and B. Stamm. *Certified reduced basis methods for parametrized partial differential equations*, volume 590. Springer, 2016.
- [29] A. Lamperti, M. Cremonesi, U. Perego, A. Russo, and C. Lovadina. A Hu–Washizu variational approach to self-stabilized virtual elements: 2D linear elastostatics. *Computational Mechanics*, 71(5):935–955, 2023.
- [30] A. Lamperti, M. Cremonesi, U. Perego, A. Russo, and C. Lovadina. A Hu–Washizu variational approach to self-stabilized quadrilateral Virtual Elements: 2D linear elastodynamics. *Computational Mechanics*, 74(2):393–415, 2024.
- [31] J. L. Lions and E. Magenes. *Non-homogeneous boundary value problems and applications: Vol. 1*, volume 181. Springer Science & Business Media, 2012.
- [32] G. Manzini, A. Russo, and N. Sukumar. New perspectives on polygonal and polyhedral finite element methods. *Mathematical Models and Methods in Applied Sciences*, 24(08):1665–1699, 2014.
- [33] F. Marcon and D. Mora. A stabilization-free virtual element method for the convection–diffusion eigenproblem. *Journal of Scientific Computing*, 102(2):1–33, 2025.
- [34] L. Mascotto. Ill-conditioning in the virtual element method: Stabilizations and bases. *Numerical Methods for Partial Differential Equations*, 34(4):1258–1281, 2018.
- [35] L. Mascotto. The role of stabilization in the virtual element method: a survey. *Computers & Mathematics with Applications*, 151:244–251, 2023.
- [36] J. Meng, X. Wang, L. Bu, and L. Mei. A lowest-order free-stabilization virtual element method for the Laplacian eigenvalue problem. *J. Comput. Appl. Math.*, 410:Paper No. 114013, 11, 2022.
- [37] D. Mora, G. Rivera, and R. Rodriguez. A virtual element method for the Steklov eigenvalue problem. *Mathematical Models and Methods in Applied Sciences*, 25(08):1421–1445, 2015.
- [38] D. Mora, G. Rivera, and I. Velásquez. A virtual element method for the vibration problem of Kirchhoff plates. *ESAIM: Mathematical Modelling and Numerical Analysis*, 52(4):1437–1456, 2018.
- [39] A. Russo and N. Sukumar. Quantitative study of the stabilization parameter in the virtual element method. In *Portugal–Italy Conference on Nonlinear Differential Equations and Applications*, pages 259–278. Springer, 2022.
- [40] M. Trezzi and U. Zerbinati. The Lightning Virtual Element Method for Self-adjoint Eigenvalue Problems. *Computational Mechanics and Applied Mathematics: Perspectives from Young Scholars: GIMC SIMAI Young 2024*, page 247.
- [41] M. Trezzi and U. Zerbinati. When rational functions meet virtual elements: the lightning virtual element method. *Calcolo*, 61(3):35, 2024.
- [42] P. Wriggers, B. D. Reddy, W. Rust, and B. Hudobivnik. Efficient virtual element formulations for compressible and incompressible finite deformations. *Computational Mechanics*, 60:253–268, 2017.

ISTITUTO DI MATEMATICA APPLICATA E TECNOLOGIE INFORMATICHE ‘E. MAGENES’, CONSIGLIO NAZIONALE DELLE RICERCHE, VIA FERRATA 5, 27100, PAVIA, ITALY

Email address: `silvia.bertoluzza@imati.cnr.it`

COMPUTER, ELECTRICAL AND MATHEMATICAL SCIENCES AND ENGINEERING DIVISION, KING ABDULLAH UNIVERSITY OF SCIENCE AND TECHNOLOGY, THUWAL 23955, SAUDI ARABIA

Email address: `fabio.credali@kaust.edu.sa`

DIPARTIMENTO DI MATEMATICA ‘F. CASORATI’, UNIVERSITÀ DEGLI STUDI DI PAVIA, VIA FERRATA 5, 27100, PAVIA, ITALY

Email address: `francesca.gardini@unipv.it`